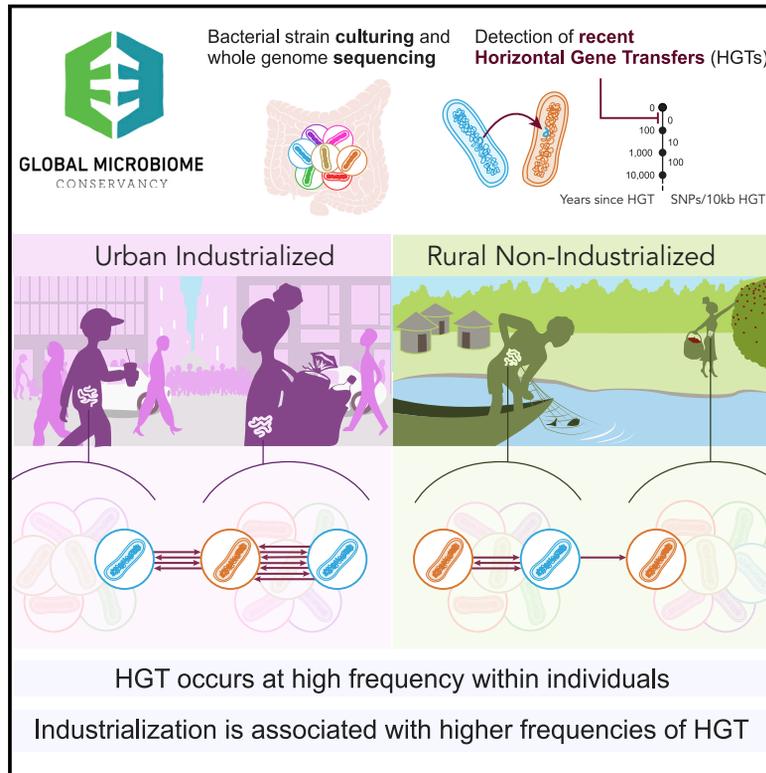## Cell

Elevated rates of horizontal gene transfer in the industrialized human microbiome

Graphical abstract

Authors

Mathieu Groussin, Mathilde Poyet, Ainara Sistiaga, ..., Roger E. Summons, Ramnik J. Xavier, Eric J. Alm

Correspondence

mgroussi@mit.edu (M.G.), mpoyet@mit.edu (M.P.), ejalm@mit.edu (E.J.A.)

In brief

A worldwide microbiome analysis from 15 populations along the industrialization gradient reveals that horizontal gene transfer occurs on short timescales and that microbiomes continuously acquire new functionality based on host lifestyle.

Highlights

- Thousands of gut bacterial genomes from worldwide human populations were sequenced

- HGT occurs at high frequency in the gut microbiome of individual persons

- HGT occurs more frequently in the microbiome of industrialized and urban populations

- Transferred gene functions in the microbiome reflect the lifestyle of the host

CellPress

Cell

Article

Elevated rates of horizontal gene transfer in the industrialized human microbiome

Mathieu Groussin,[1,2,3,4,38,*] Mathilde Poyet,[1,2,3,4,38,*] Ainara Sistiaga,[4,5,6] Sean M. Kearney,[1,2] Katya Moniz,[1,2,4] Mary Noel,[4,7] Jeff Hooker,[4,7] Sean M. Gibbons,[4,8,9] Laure Segurel,[4,10,39] Alain Froment,[4,11] Rihlat Said Mohamed,[12] Alain Fezeu,[4,13] Vanessa A. Juimo,[4,13] Sophie Lafosse,[10] Francis E. Tabe,[14] Catherine Girard,[4,15,16] Deborah Iqaluk,[4,17] Le Thanh Tu Nguyen,[1,2,3,4] B. Jesse Shapiro,[4,15,18,19] Jenni Lehtimäki,[4,20,21] Lasse Ruokolainen,[4,20] Pinja P. Kettunen,[4,20]

(Author list continued on next page)

[1]Department of Biological Engineering, Massachusetts Institute of Technology, Cambridge, MA, USA
[2]Center for Microbiome Informatics and Therapeutics, Massachusetts Institute of Technology, Cambridge, MA, USA
[3]The Broad Institute of MIT and Harvard, Cambridge, MA, USA
[4]The Global Microbiome Conservancy, Massachusetts Institute of Technology, Cambridge, MA, USA
[5]Department of Earth, Atmospheric and Planetary Science, Massachusetts Institute of Technology, Cambridge, MA, USA
[6]GLOBE Institute, University of Copenhagen, Copenhagen, Denmark
[7]Chief Dull Knife College, Lame Deer, MT, USA
[8]Institute for Systems Biology, Seattle, WA, USA
[9]Department of Bioengineering, University of Washington, Seattle, WA, USA
[10]UMR7206 Eco-anthropologie, CNRS-MNHN-Univ Paris Diderot-Sorbonne, Paris, France
[11]Institut de Recherche pour le Développement UMR 208, Muséum National d'Histoire Naturelle, Paris, France
[12]SA MRC / Wits Developmental Pathways for Health Research Unit, Department of Paediatrics, School of Clinical Medicine, Faculty of Health Sciences, University of Witwatersrand, Johannesburg, South Africa
[13]Institut de Recherche pour le Développement, Yaounde, Cameroon
[14]Faculté de Médecine et des Sciences Biomédicales, Université Yaoundé 1, Yaoundé, Cameroun
[15]Université de Montréal, Département de sciences biologiques, C.P. 6128, succursale Centre-ville, Montréal, QC, Canada
[16]Centre d'études nordiques, Département de biochimie, de microbiologie et de bio-informatique, Université Laval, 1030 rue de la Médecine, Québec, QC, Canada
[17]Resolute Bay, Nunavut, Canada
[18]Department of Microbiology and Immunology, McGill University, Montreal, QC, Canada
[19]McGill Genome Centre, McGill University, Montreal, QC, Canada
[20]Organismal and Evolutionary Biology Research Programme, Faculty of Biological and Environmental sciences, University of Helsinki, Helsinki, Finland
[21]Environmental Policy Centre, Finnish Environment Institute SYKE, Helsinki, Finland

(Affiliations continued on next page)

SUMMARY

Industrialization has impacted the human gut ecosystem, resulting in altered microbiome composition and diversity. Whether bacterial genomes may also adapt to the industrialization of their host populations remains largely unexplored. Here, we investigate the extent to which the rates and targets of horizontal gene transfer (HGT) vary across thousands of bacterial strains from 15 human populations spanning a range of industrialization. We show that HGTs have accumulated in the microbiome over recent host generations and that HGT occurs at high frequency within individuals. Comparison across human populations reveals that industrialized lifestyles are associated with higher HGT rates and that the functions of HGTs are related to the level of host industrialization. Our results suggest that gut bacteria continuously acquire new functionality based on host lifestyle and that high rates of HGT may be a recent development in human history linked to industrialization.

INTRODUCTION

Transitioning from nonindustrialized to industrialized lifestyles is associated with changes in gut microbiome composition and decreased bacterial species diversity (Brewster et al., 2019; Hansen et al., 2019; McDonald et al., 2018; Pasolli et al., 2019; Schnorr et al., 2014; Sonnenburg and Sonnenburg, 2019b; Yatsunenko et al., 2012). While the precise causes of these changes are unknown, factors associated with the development of industrialized societies such as sanitation, the consumption of

Tommi Vatanen,[3,4,22] Shani Sigwazi,[4,23] Audax Mabulla,[4,24] Manuel Domínguez-Rodrigo,[4,25,26] Yvonne A. Nartey,[4,27] Adwoa Agyei-Nkansah,[4,28] Amoako Duah,[4,29] Yaw A. Awuku,[4,30] Kenneth A. Valles,[4,31] Shadrack O. Asibey,[4,32] Mary Y. Afihene,[4,33] Lewis R. Roberts,[4,34] Amelie Plymoth,[4,27] Charles A. Onyekwere,[4,35] Roger E. Summons,[4,5] Ramnik J. Xavier,[3,4,36,37] and Eric J. Alm[1,2,3,4,40,*]

[22]The Liggins Institute, University of Auckland, Auckland 1023, New Zealand
[23]Tumaini University Makumira, Arusha, Tanzania
[24]Department of Archaeology and Heritage Studies, University of Dar es Salaam, Tanzania
[25]Prehistory Unit, Department of History and Philosophy, University of Alcalá, Alcalá de Henares, Madrid, Spain
[26]Institute of Evolution in Africa, University of Alcalá de Henares, Madrid, Spain
[27]Department of Medical Epidemiology and Biostatistics, Karolinska Institutet, Stockholm, Sweden
[28]Department of Medicine and Therapeutics, University of Ghana Medical School and Korle Bu Teaching Hospital, Accra, Ghana
[29]Department of Medicine, St. Dominic Hospital, Akwatia, Ghana
[30]Department of Internal Medicine and Therapeutics, School of Medical Sciences University of Cape Coast, Cape Coast, Ghana
[31]Medical Scientist Training Program, Mayo Clinic, Rochester, 55905, USA
[32]Catholic University College, Sunyani, Ghana
[33]Department of Medicine, Kwame Nkrumah University of Science and Technology, Kumasi, Ghana
[34]Division of Gastroenterology and Hepatology, Mayo Clinic, 200 First Street SW, Rochester, MN, USA
[35]Department of Medicine, Lagos State University College of Medicine, Lagos, Nigeria
[36]Center for Computational and Integrative Biology, Massachusetts General Hospital and Harvard Medical School, Boston, MA, USA
[37]Department of Molecular Biology, Massachusetts General Hospital, Boston, MA, USA
[38]These authors contributed equally
[39]Present address: Laboratoire de Biométrie et Biologie Evolutive UMR5558, CNRS - Université Lyon 1, Université de Lyon, Villeurbanne, France
[40]Lead contact
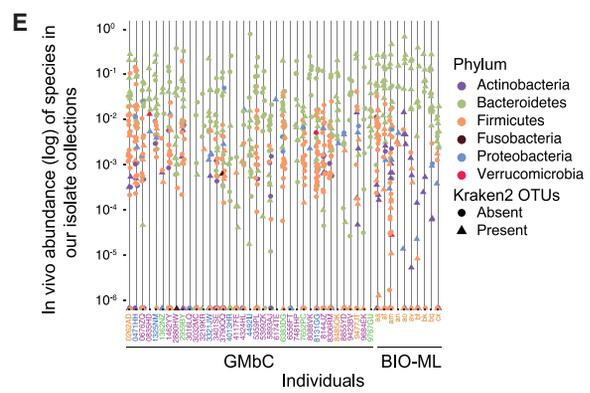*Correspondence: mgroussi@mit.edu (M.G.), mpoyet@mit.edu (M.P.), ejalm@mit.edu (E.J.A.)
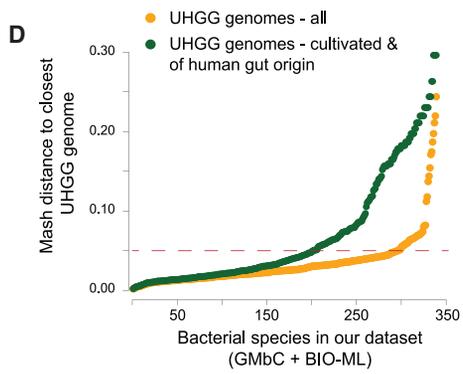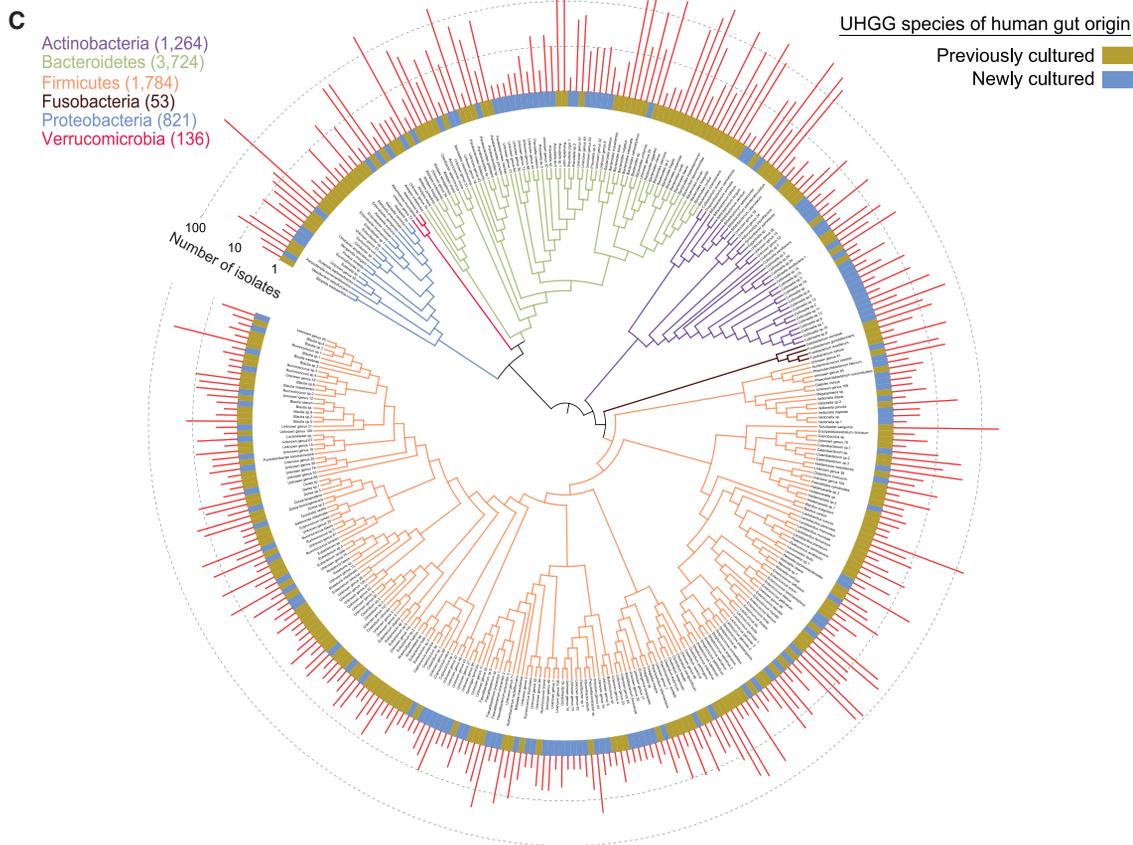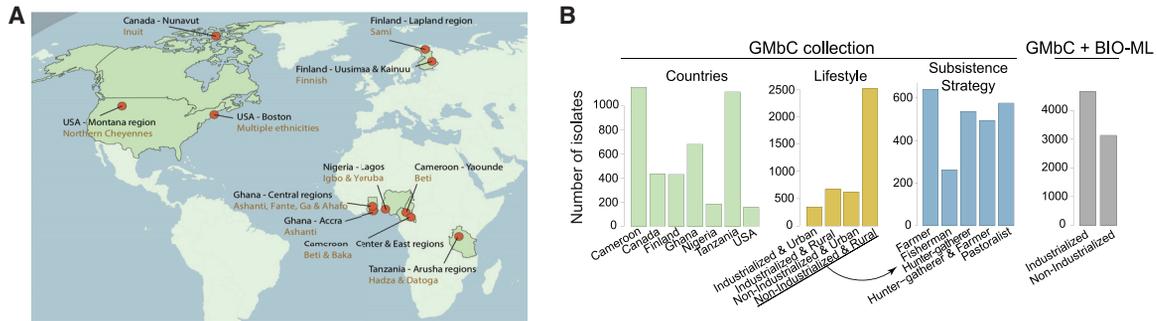https://doi.org/10.1016/j.cell.2021.02.052

processed food, higher frequency of caesarean section, and increased use of antibiotics likely play key roles in remodeling the gut microbiome (Sonnenburg and Sonnenburg, 2019a). These perturbations in the gut ecosystem can occur shortly after individuals transition from nonindustrialized to industrialized areas and persist for years (Vangay et al., 2018), further confirming that lifestyle strongly influences the function of our gut microbiome. However, the effects of host and environmental factors associated with industrialized lifestyles on individual gut bacterial genomes are poorly characterized.

Bacteria can use horizontal gene transfer (HGT) to adapt rapidly to unstable environments through the acquisition of new functions. Mammalian gut bacteria have experienced frequent HGT events over millions of years of evolution (Hehemann et al., 2010; Smillie et al., 2011). Previous studies of specific bacterial species showed that HGT can occur and be conserved in the gut microbiome within a single individual (Coyne et al., 2014; Garud et al., 2019; Munck et al., 2020; Yaffe and Relman, 2020; Zhao et al., 2019; Zlitni et al., 2020), especially when there is strong selection for target functions such as antibiotic resistance (Forsberg et al., 2012; Lopatkin et al., 2017; Modi et al., 2013). Yet, it remains unclear whether HGT can occur broadly enough to impact gut microbiome function over an individual's lifetime, such as in response to significant lifestyle changes, or whether microbiomes primarily acquire new functions through the acquisition of new strains. It was previously observed that individual bacterial strains can reside within a host microbiome for decades (Faith et al., 2013). If the rate of gene transfer is sufficiently rapid, then a microbiome that is "stable" in terms of bacterial populations (Faith et al., 2013; Gibbons et al., 2017; Mehta et al., 2018) could nonetheless evolve in response to host-specific environmental perturbations through HGT, perhaps in response to changes in host lifestyle.

In a previous study (Smillie et al., 2011), we found high levels of HGTs in the human microbiome involving >500-bp-length sequences with >99% similarity. Those results lacked the temporal resolution and the diversity in human populations necessary to address the questions of timescales and host lifestyle. Over short evolutionary timescales, the substitution rate of many bacterial species typically falls in the range of ~1 SNP/genome/year (Didelot et al., 2016; Drake, 1991; Duchêne et al., 2016; Zhao et al., 2019). Assuming this rough molecular clock approximation, and a genome size of 10^6 bp, the HGTs we detected using those criteria (>500 bp, >99% similarity) were consistent with transfer events that occurred between 0 and 10,000 years ago (see STAR Methods). Variations in the molecular clock across species and genomic regions may shorten or expand this time interval. In any case, our previous results could not constrain the dates of HGT that occurred more recently than the rise of modern industrialization, dated to the 18th–19th century (de Vries, 1994). To answer the question of whether commensal strains can frequently acquire new functionality through HGT within an individual, such that recent adaptations to industrialization are detectable in contemporary bacterial genomes, more precise estimates of the rate and extent of HGT are needed.

Existing reference isolate genomes (Browne et al., 2016; Faith et al., 2013; Forster et al., 2019; Goodman et al., 2011; Zou et al., 2019) originate almost exclusively from industrialized populations and, for the vast majority of strains, from different individuals, making investigation of within-person HGT impossible. Here, we present the Global Microbiome Conservancy (GMbC) isolate collection, composed of >4,000 cultured, isolated, and sequenced gut bacteria from diverse industrialized and nonindustrialized populations, including rich sets of strains from single individuals. We used these genomes to investigate the rate and patterns of gene transfers that occurred very recently in human history. We show that HGTs can occur at high and

A — Map of sampling locations

Canada - Nunavut
Inuit

Finland - Lapland region
Sami

Finland - Uusimaa & Kainuu
Finnish

USA - Montana region
Northern Cheyennes

USA - Boston
Multiple ethnicities

Nigeria - Lagos
Igbo & Yoruba

Cameroon - Yaounde
Beti

Ghana - Central regions
Ashanti, Fante, Ga & Ahafo

Ghana - Accra
Ashanti

Cameroon
Center & East regions
Beti & Baka

Tanzania - Arusha regions
Hadza & Datoga

B

GMbC collection

Countries
Lifestyle
Subsistence Strategy

GMbC + BIO-ML

Number of isolates

Cameroon, Canada, Finland, Ghana, Nigeria, Tanzania, USA

Industrialized & Urban
Industrialized & Rural
Non-Industrialized & Urban
Non-Industrialized & Rural

Farmer
Fisherman
Hunter-gatherer
Hunter-gatherer & Farmer
Pastoralist

Industrialized
Non-Industrialized

C

Actinobacteria (1,264)
Bacteroidetes (3,724)
Firmicutes (1,784)
Fusobacteria (53)
Proteobacteria (821)
Verrucomicrobia (136)

UHGG species of human gut origin

Previously cultured
Newly cultured

Number of isolates
100
10
1

D

UHGG genomes - all
UHGG genomes - cultivated & of human gut origin

Mash distance to closest UHGG genome

0.30
0.20
0.10
0.00

50   150   250   350

Bacterial species in our dataset (GMbC + BIO-ML)

E

In vivo abundance (log) of species in our isolate collections

10^0
10^{-1}
10^{-2}
10^{-3}
10^{-4}
10^{-5}
10^{-6}

Phylum
Actinobacteria
Bacteroidetes
Firmicutes
Fusobacteria
Proteobacteria
Verrucomicrobia

Kraken2 OTUs
Absent
Present

GMbC   BIO-ML

Individuals

(legend on next page)

heterogeneous frequency within individuals, and we report elevated rates of gene transfer in industrialized populations.

RESULTS

A diverse collection of bacterial isolate genomes from worldwide gut microbiomes

We cultured, isolated, and whole-genome sequenced 4,149 gut bacteria from 37 individuals from 14 distinct populations with different levels of industrialization (Figures 1A and 1B). Bacteria were isolated from stool samples under anaerobic conditions, using previously published protocols (Poyet et al., 2019). We combined these GMbC genomes with a set of 3,632 isolate genomes from the Broad Institute-OpenBiome Microbiome Library (BIO-ML) genome collection that we recently generated from 11 urban American donors (Poyet et al., 2019), yielding a dataset of 7,781 isolate genomes. We then divided our cohort of 48 individuals according to two different parameters, which we defined as: "urban" versus "rural" (based on local population density) (SEDAC Population Estimation Service, 2015), and "industrialized" versus "nonindustrialized" (based on the Human Development Index [HDI] at the country level) (United Nations Development Program, 2020). For the purposes of this analysis, we used HDI as a proxy for industrialization because it reflects parameters that are relevant to health and the microbiome, such as the consumption of processed foods, rates of noncommunicable diseases, sanitation infrastructure, and health expenditure (United Nations Development Program, 2020). This classification system yielded four groups of different lifestyles: rural nonindustrialized, urban nonindustrialized, rural industrialized, and urban industrialized (see Figures 1A, 1B, S1A, and S1B and Table S1 for descriptions of population metadata and microbiome compositions). The nonindustrialized rural cohort includes populations with diverse subsistence strategies, including hunter-gatherers, pastoralists, fishermen, and farmers (Figure 1B).

We grouped our 7,781 isolate genomes into species clusters based on genomic similarity, using the Mash distance as a proxy for average nucleotide identity (see STAR Methods). This identified 339 bacterial species across 6 phyla, grouping into 73 known and 88 unknown genera (see Figure 1C and Table S2 for culturing data and genome assembly statistics). Comparing our genome collection to the Unified Human Gastrointestinal Genome (UHGG) database (see STAR Methods; Almeida et al.,

2021), which comprises the largest set of human gut bacterial genomes, we found that 13% of the species in our collection have no representatives among all characterized UHGG species (which include species defined from metagenomic data alone), and 41% have no representatives among the set of previously cultivated human gut species (Figure 1D). We sampled a median of 93 isolate genomes and 17 species per individual, covering a wide range of within-person bacterial taxonomies and *in vivo* abundances (Figure 1E; Table S1), providing within-person genomic and ecological diversity for high-resolution investigation of HGTs.

Individual gut microbiomes harbor extensive recent HGTs

We first detected and quantified HGT events that occurred recently in human history. We screened all genomes for large blocks of 100% identical DNA that were shared between any pairs of genomes of different species, retaining blocks larger than 500 bp (hereafter named "500bp+ HGTs") or larger than 10 kb ("10kb+ HGTs"). HGT is the best explanation for these observations compared to vertical inheritance, as the expected number of mutations between highly conserved and vertically inherited ribosomal genes of different species far exceeds the threshold (0 SNP) used in our heuristic to retain candidate HGTs (Figure S1C). 10-kb+ HGTs that do not contain any mutations correspond to events that occurred between 0 and ~100 years ago (see STAR Methods). Thus, these 10kb+ HGTs likely occurred over the most recent two or three human generations, including within the sampled individuals. We removed putative contaminants from the analysis by filtering out HGTs with low relative sequencing coverage (i.e., compared to the coverage of the two genomes under consideration; see STAR Methods), resulting in a set of HGTs with median relative coverage of 1.13 (Figure S1D). We found that 90% (7,031/7,781) and 53% (4,096/7,781) of our genomes are involved in at least one 500bp+ HGT and one 10kb+ HGT, respectively (Figure 2A; Table S3), covering a diversity of taxonomic groups (Figure 2B). HGTs included genes that are involved in a variety of cellular, metabolic, and informational functions (Figure S1E), with selfish element and phage/conjugative transposon functions being enriched in the set of 500bp+ HGTs and 10kb+ HGTs, respectively (Figure S1F). Many of the genes carried by within-person 10kb+ HGTs segregate at high frequencies in bacterial populations

Figure 1. Assembly of a geographically, phylogenetically, and ecologically diverse collection of human gut bacterial isolate genomes

(A) Samples were collected from 15 communities in the USA, Canada, Finland, Cameroon, Tanzania, Ghana, and Nigeria. Red dots show the geographic locations of sampling sites. Participants represented four different lifestyle categories: 14 urban industrialized (UI) individuals in the USA and eastern and southern Finland; 5 rural industrialized (RI) individuals in the USA, arctic Finland, and the Canadian arctic; 6 urban nonindustrialized (UN) individuals in Cameroon, Nigeria, and Ghana; and 23 rural nonindustrialized (RN) individuals in Cameroon, Tanzania, and Ghana. See Table S1 for further individual metadata.

(B) Distribution of isolate genomes across countries, lifestyles, and subsistence strategies.

(C) Phylogenetic tree of representative genomes of all 339 species in our isolate genome collections (GMbC + BIO-ML). The inner ring shows species that, prior to our work, did not have representative genomes among the cultured bacteria of human gut origin in the UHGG database. The outer ring shows the distribution of genomes across all species in the GMbC + BIO-ML collection.

(D) Genomic distance between each representative genome of the GMbC + BIO-ML collection and the closest representative in the UHGG database. Orange dots show results with all UHGG genomes, which includes metagenome-assembled genomes (MAGs). Green dots show comparisons only with genomes from cultivated bacteria of human gut origin. The red dash line shows the threshold (D = 0.05) that is classically used to delineate species.

(E) *In vivo* abundance of all species in the GMbC + BIO-ML collection. Individuals are colored by lifestyle category (UI in orange, RI in green, UN in blue, and RN in purple). Species that were not detected by Kraken2 (low abundance or no close representatives in genome collections) are shown as dots; species detected by Kraken2 are shown as triangles.
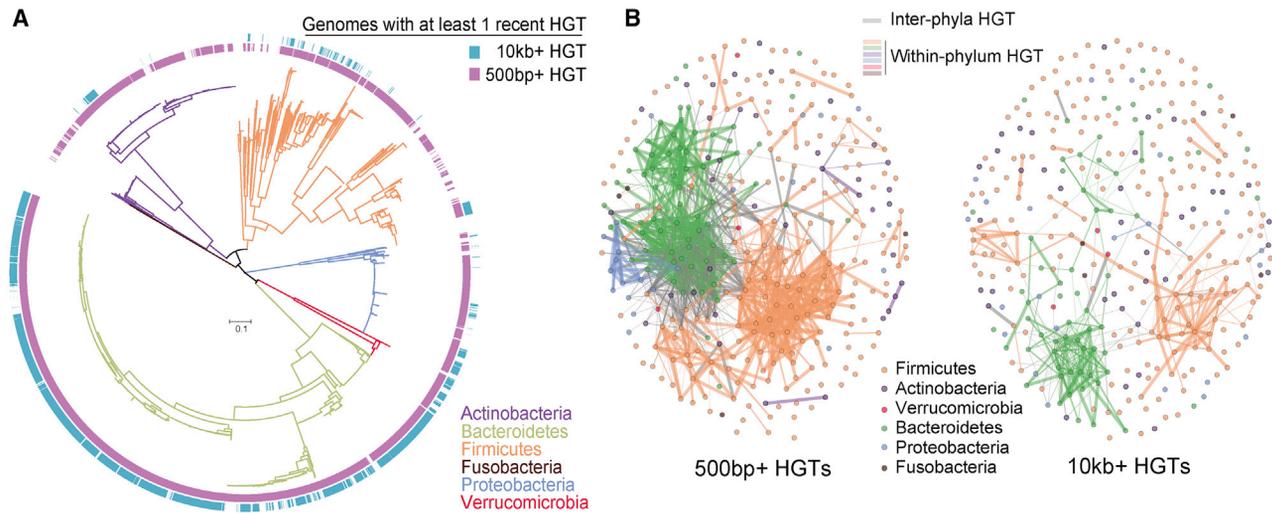
Figure 2. Diverse human gut bacteria recently engaged in frequent HGT

(A) Phylogenomic tree of the 7,781 human gut bacterial isolates that we analyzed in this study, which were sampled from 15 human populations. The tree has been reconstructed by maximum likelihood with a multiple sequence alignment of ribosomal protein-coding genes. Branches are colored by phylum and branch lengths are expressed in expected number of substitutions per site. The inner (purple) and outer (blue) rings show genomes in which at least 1 HGT larger than 500 bp and 10 kb was detected, respectively.

(B) Networks of within-person HGT frequency derived from 500bp+ (left) and 10kb+ (right) HGTs. Vertices represent bacterial species and are colored by phylum. Edge width is proportional to the average within-person HGT frequency between the two connected species. Colored edges show within-phylum HGTs, while gray edges represent between-phylum HGTs.

within each host, suggesting potential fixation (Figure S1G). However, the majority of transferred genes are found at low frequency, reflecting their recent acquisition in the population (Figure S1G).

To test whether these HGTs occurred recently, we compared the frequency and count of 10kb+ HGTs observed between bacteria isolated from a single individual with that observed between the same bacteria from different individuals (see STAR Methods). We hypothesized that if transfers occur frequently within individual microbiomes, then we would observe higher levels of transfer between strains isolated from a single host. Alternatively, if transfers rarely occur (i.e., at rates slower than strain turnover), then we would observe similar levels of HGT between bacteria regardless of whether they were isolated from the same host. Importantly, both within-person and between-people HGTs include some background level of more ancient HGT (e.g., very slowly evolving genomic regions that are still 100% similar over the 10kb+ region) that do not result from direct sharing between two co-residing species in present microbiomes. Bacterial species that share genes directly, however, will only be found in within-person comparisons. The difference between the within-person and between-people HGTs reflects the very recent HGTs that occurred within individuals and thus can be quantified. We found that bacterial species pairs sampled within individuals are more likely to share recently transferred DNA than the same species pairs sampled from two different people; using a Poisson distribution, we compared the observed count of HGT events for pairs of species sampled within individual people to its expected value based on HGT frequencies of the same species pairs found between people (Figure 3A; p value < 2.2×10^{-308}). This comparison allows us to correct for differences in the num-

ber of both genome and individual pairs being sampled between the two categories (within person versus between people) (see statistical analyses in STAR Methods). We also randomly downsampled our data to further control for the unequal sampling of genomes across individual pairs (see statistical analyses in STAR Methods), which confirmed that observed HGT counts within individual people are higher than expected HGT counts (100 random replicates, Welsh t test, t = 259.56, df = 102.44, p value = 3.3×10^{-146}; see Table S4).

We next controlled for the effect of phylogeny on this result, as more closely related species are more likely to engage in HGT (Smillie et al., 2011) and could be unevenly distributed between within-person and between-people categories. In our data, phylogenetic relatedness strongly associates with HGT frequency (generalized linear mixed effects [GLME] models; n (species pairs) = 3,667; odds ratio [OR] = 0.02; 95% confidence interval [CI] = 0.01–0.06; combined with a likelihood ratio test ([LRT], χ^2 = 62.96; p value = 2.1×10^{-15}) but does not confound our result; the within-person HGT is significantly higher than the between-people HGT across phylogenetic distance bins (Fisher's method; χ^2 = 204.5 and p value = 7×10^{-28} for 10kb+ HGTs; χ^2 = 149.1 and p value = 1.8×10^{-14} for 500bp+ HGTs) (Figure 3B). In addition, the higher levels of within-person HGTs are also observed when looking at the larger set of 500bp+ HGTs (Poisson distribution, p value < 2.2×10^{-308}) (Figures 3A and S2J). We also investigated whether the higher within-person HGT that we observed at the aggregate level was present in individual populations as well. Performing our analyses for each of the sampled countries or ethnic groups containing more than four individuals separately, we found that this observation was replicated in each individual group (Figures S2A–S2I). In

A

10kb+ HGTs

Within-person HGT counts

10kb+ HGTs   500bp+ HGTs

p-value < 2.2 x 10⁻³⁰⁸

B

10kb+ HGTs
Within-people
Between-people

p = 7 x 10⁻²⁸

500bp+ HGTs
Within-people
Between-people

p = 1.8 x 10⁻¹⁴

C

Probability distribution of vertical strain transmission
Beta - β(2, 11)
Beta - β(2, 2)

D

E

Bacteroides vulgatus

F

G
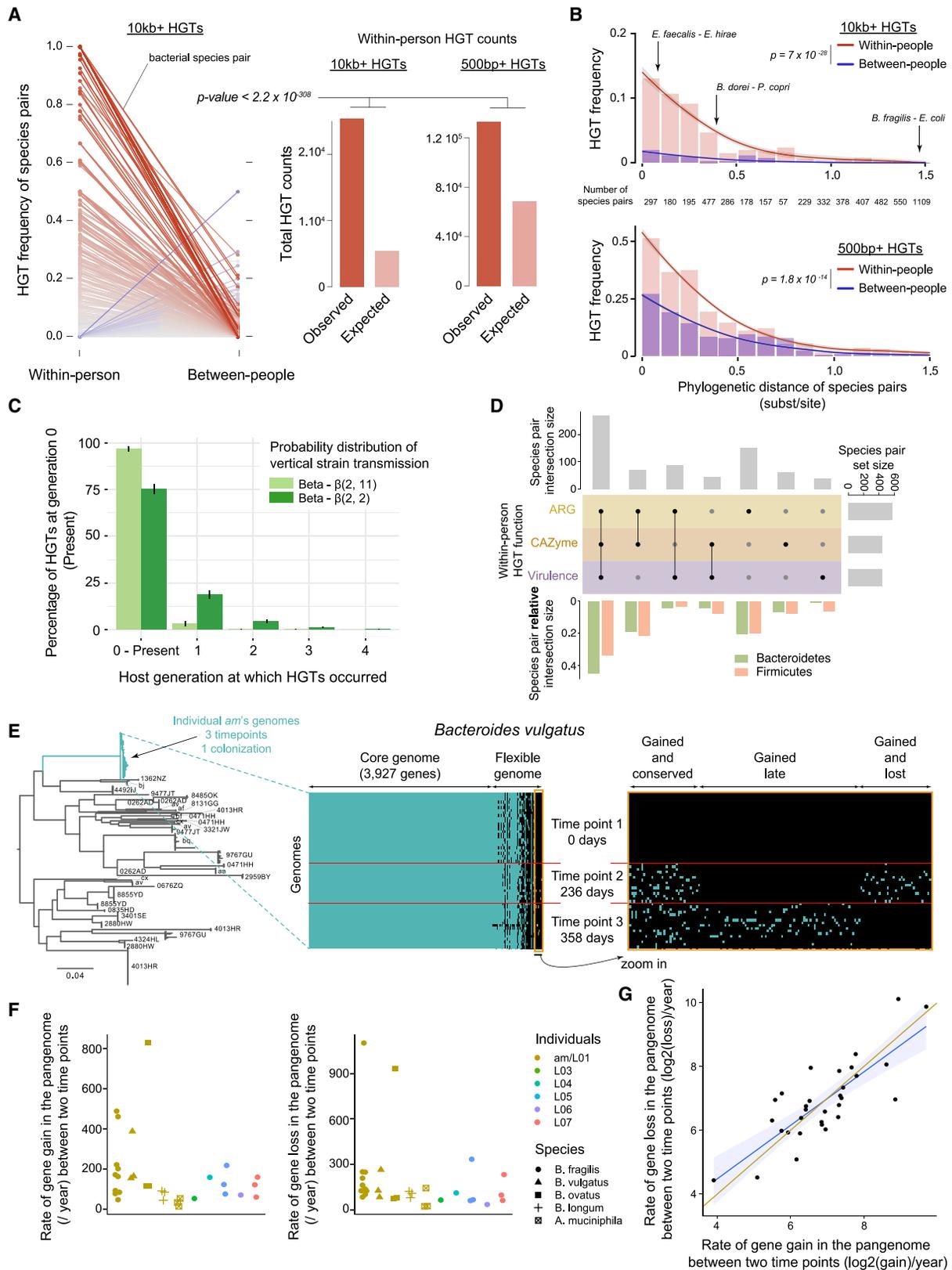
(legend on next page)

addition, we controlled for the effect of the *in vitro* culturing of bacteria on the quantification of HGTs, as bacteria co-cultured on the same plate or in the presence of antibiotics could experience HGTs that do not reflect *in vivo* events. We did not find any significant increase in HGT for genome pairs grown on the same plate or in the presence of antibiotics (see STAR Methods and Table S4 for all statistical comparisons).

The signal of HGT enrichment within individuals compared to its expected value suggests that a broad and diverse set of bacterial species very recently engaged in HGT and that HGTs can rapidly accumulate in bacterial pangenomes. Strictly speaking, we cannot yet distinguish between individual transfers that occurred in the host of origin from those that may have occurred in a host's parent or even grandparent. However, host intergenerational co-transmission of species involved in past HGTs must occur to observe ancient HGT events in today's microbiome. To be counted in our analyses, these HGTs must also not experience any mutation. We used a simulation approach to quantify the amount of HGTs in the host of origin (generation 0, sampled at present time) that would represent past HGT events originating from previous generations and that would not have experienced any mutation (see STAR Methods). We used a previously published rate of mother-to-infant strain transmission, estimated to be ~16% (Ferretti et al., 2018), to fix the rate of intergenerational species transmission in our simulations. We also simulated data using a more extreme rate of 50% of species transmission across generations. We found that the number of HGTs rapidly decays across generations (Figure 3C). In total, the amount of 100% similar HGTs observed at present generation that originate from ancient generations is ~3% with the 16% probability of vertical species transmission and ~25% when considering the extreme probability of 50% species transmission. These results strongly suggest that the vast majority of HGTs being seen in within-person species comparisons occurred during the present generation (i.e., during the lifetime of each sampled individual).

We next investigated whether, within people, bacterial species engage in the transfer of gene functions that may impact bacterial metabolism or host physiology. To test this, we looked at within-person transferred genes involved in antibiotic resistance (antibiotic resistance genes [ARGs]), carbohydrate degradation (carbohydrate active enzyme [CAZyme]), and virulence. We found hundreds of species pairs engaging in the transfer of at least one of these three functions, with the majority of species pairs exchanging multiple functions (Figure 3D), an observation relevant to both Firmicutes and Bacteroides species pairs (Figure 3D).

Bacterial species acquire genes at high and heterogenous frequency within individual people

Next, we hypothesized that if bacteria frequently acquire new genes within each person, then their pangenomes should exhibit strong variations in gene content over time. To directly measure the rate of within-person gene acquisition, we analyzed the gene repertoires of isolate genomes that were longitudinally sampled over the course of ~6–18 months in two previous studies: 198 isolate genomes from five species (*Bacteroides fragilis*, *Bacteroides vulgatus*, *Bacteroides ovatus*, *Bifidobacterium longum*, and *Akkermansia muciniphila*) sampled in one individual (Poyet et al., 2019) and 191 *Bacteroides fragilis* isolate genomes sampled in five additional people (Zhao et al., 2019; Figures 3E and S3; Table S5). As strain replacement between time points can contribute to pangenome diversity, we used SNPs and phylogenetic reconstructions to restrict our quantification of the dynamics of gene repertoires to clades of closely related genomes that diversified within their host following initial colonization of the gut (see STAR Methods, Figures 3E and S3, and phylogenetic trees reconstructed in Zhao et al., 2019). We also controlled for differences in genome set sizes and genome coverage between time points (see STAR Methods and Figure S3J) and accounted for read coverage information at the individual gene level to derive the final gene presence/absence profile of a given genome (see STAR Methods). We first quantified the rates at which new genes are gained in the pangenome of these five species between any two time points. For each

Figure 3. HGTs accumulate rapidly within the gut microbiome of individual people

(A) HGT frequencies within and between people were computed using the whole set of 7,781 genomes and were averaged across all within-person and between-people pairs, respectively. Each solid line represents a bacterial species pair sampled both within and between individuals and connects HGT frequencies in the two categories of pairs of individuals. The order in which lines are displayed is at random. Differences in HGT frequency are colored along a gradient from gray (no difference) to red (within-person HGT frequency is higher than between-people) or from gray to blue (between-people HGT frequency is higher than within-person), with darker colors representing greater differences. Barplots show the observed total HGTs for bacterial species pairs found within individuals, compared to their expected values (see STAR Methods). The number of species and genome pairs for each comparison are listed in Table S3.

(B) Association between HGT frequency and phylogenetic distance of species pairs (LOESS regression; distances derived from the tree in Figure 2A, expressed in aa/site; bands represent confidence intervals calculated from the standard errors). Bars show the average HGT frequencies across all species pairs in each bin. Within-person HGT frequencies are compared to between-people HGTs with the Fisher's method to combine p values (see STAR Methods).

(C) Host generation in which observed HGTs detected in the microbiome in generation 0 (present time) occurred in our simulation. Light and dark bars show results obtained when setting the intergenerational transmission of bacterial species to 16% and 50%, respectively. Error bars represent standard deviations for calculated HGT percentages.

(D) "Upset" plot showing the intersections between the sets of species pairs involved in within-person HGTs of ARG, CAZyme, and virulence genes. Barplots in the bottom show the relative intersection sizes for Firmicutes and Bacteroidetes species pairs.

(E) Within-person acquisition of genes in *Bacteroides vulgatus* genomes over the course of 358 days. The tree depicts the relationships between all *B. vulgatus* isolates sampled across all individuals in our dataset, with isolates in blue being longitudinally sampled in individual "*am*". IDs of other individual hosts are shown. Middle and right panels show gene presence/absence in *am* genomes (rows), sorted by sampling times. The right panel is a zoom-in of the set of gene families that were absent in the pangenome at the first time point. See Figure S3 and Table S5 for data and results on additional species.

(F) Within-person rates of gene gain (left) and loss (right) in the pangenome (expressed as number of events/year).

(G) Correlation between within-person rates of gene gain and gene loss in pangenomes. The blue line represents the linear regression between gene gain and loss. The yellow line shows the y = x line.

species in a single individual, we found that the rate of gene acquisition in the pangenome is heterogeneous over time (Figure 3F), varying from tens to hundreds of gene gains per year. This suggests that gene transfers do not accumulate in a clock-like fashion, probably because one HGT event can include a single gene or a large plasmid. Our results further show that average rates of gene gain in the pangenome per year are heterogeneous across species; Bacteroides species acquire new genes in their pangenome at higher rates compared to *B. longum* and *A. muciniphila* (238 ± 132 genes/year for *B. vulgatus*, 353 ± 412 genes/year for *B. ovatus*, and 161 ± 124 genes/year for *B. fragilis* compared to 74 ± 25 genes/year for *B. longum* and 34 ± 20 genes/year for *A. muciniphila*) (Figure 3F; Table S5). These rates, which are directly estimated from longitudinal data, mirror those calculated from our cross-sectional inference in Figure 3A. Using the set of within-person HGTs, we calculated the average HGT frequency across all genome pairs involving either *B. vulgatus*, *B. ovatus*, *B. fragilis*, *B. longum*, and *A. muciniphila*. We confirmed that Bacteroides species engage more frequently in HGT compared to *B. longum* and *A. muciniphila*, with average HGT frequencies equal to 2.2%, 2.3%, 0.85%, 0.04%, and 0.06% for 10kb+ HGTs in *B. vulgatus*, *B. ovatus*, *B. fragilis*, *B. longum*, and *A. muciniphila*, respectively, and 8.6%, 10.1%, 6.0%, 0.81%, and 1.64% for 500bp+ HGTs, respectively. As expected, rates of gene gains are strongly correlated with rates of gene loss (Figure 3G; Spearman correlation, S = 1,188, rho = 0.76, p value = 2.3×10^{-6}), ultimately maintaining overall proteome sizes (Mira et al., 2001). Altogether, our results suggest that a variety of gene functions are horizontally exchanged in the gut microbiome of each individual host and at rates that may be sufficiently high to reshape the functions of gut bacterial populations during an individual's lifetime.

HGT occurs at higher frequency in the gut microbiomes of industrialized populations

Having found that HGT occurs frequently within individuals, we next investigated the extent to which HGT rates and functions vary across human populations that have different levels of industrialization. For this, we looked at the bacterial species pairs in our dataset that are shared by pairs of population groups along our gradient of industrialization and urbanization, which comprises four lifestyle categories (Figure 4A; Tables S1 and S6). This approach allowed us to compare populations with both major and more modest differences in lifestyle. This analysis also restricts HGT comparisons to species pairs that are shared between two host populations. As a consequence, we used a more inclusive definition of HGT (the set of 500bp+ HGTs) for this analysis to make up for the loss of statistical power that resulted from comparing populations two at a time.

We found that species pairs sampled in the urban industrialized populations exchanged genes more frequently than when they occurred in the rural nonindustrialized group. The number of observed HGTs found in species pairs of the urban industrialized group was compared to the expected number of events, based on the HGT frequency of the same species pairs in the rural nonindustrialized populations (p value < 2.2×10^{-308}) (Figure 4B). These results hold whether averaging both within-per-

son and between-people HGTs or only within-person HGTs (Figure 4B). We also randomly downsampled the data to control for the unequal sampling of genomes across individual pairs (see statistical analysis in STAR Methods), which confirmed that observed HGT counts in the urban industrialized group are higher than expected HGT counts (100 random replicates, Welsh t test, t = 225.04, degrees of freedom [df] = 154.8, p value = 1.2×10^{-196}; see Table S4). To check whether these effects were driven by outlier individuals rather than population-level differences, we shuffled membership of individuals across groups (either by shuffling the lifestyles of individuals or pairs of individuals) and re-ran the analysis; the true urban industrialized cohort still had significantly higher rates of HGT than the randomly created groups (1,000 permutations each, p values < 0.001; see Figure S4). This effect also holds when restricting the analysis to each type of subsistence strategy (e.g., hunter-gatherer, pastoralist, or farmer) within the rural nonindustrialized cohort, which we compared individually to the urban industrialized group (Figures S5A–S5D).

Along our lifestyle gradient (Figure 4A), we consistently found that HGTs are much more frequent among the industrialized and/or urban populations across all pairwise group comparisons (Figures 4C and S5E). This effect was observed across different comparison metrics, such as the average difference in HGT frequency and the count and proportion of species pairs with higher HGT frequency (Figures 4D–4F).

We then controlled for different microbial and ecological factors that could confound this effect of lifestyle on HGT frequencies, such as bacterial phylogeny, bacterial cell wall architecture, and, more importantly, differences in species abundances between cohorts. We hypothesized that pairs of highly abundant species in a given ecosystem would have a higher probability of gene exchange compared to pairs involving at least one low-abundance species, independent of their phylogenetic distance. This hypothesis has never been directly tested, because datasets that paired in-depth genomic sampling with accurate abundance estimates did not yet exist. To test the abundance hypothesis, we calculated the average abundance of each bacterial species within each person (see STAR Methods and Figure 1E). To test for the effect of cell wall architecture, we used reference Gram staining data for each bacterial species as a proxy of cell wall architecture. We used GLME models combined with LRTs on the complete dataset to measure the effect of host lifestyle on HGT frequencies while also accounting for the aforementioned factors (see STAR Methods). We confirmed a significant association between lifestyle and HGT frequency (n (species pairs) = 10,104; OR for the industrialized lifestyle = 1.99; 95% CI = 1.96–2.03; LRT, χ^2 = 6629.4, p value < 2.2×10^{-308}). We also found that species abundance is a strong determinant of HGT (n = 10,104; OR for lowly abundant species = 0.40; 95% CI = 0.39–0.43; LRT, χ^2 = 3225.4, p value < 2.2×10^{-308}), even after accounting for the effect of other factors in the GLME models (Figure 5A). Abundant bacteria are more likely to engage in HGT with other abundant bacteria, which is consistent with the canonical mechanisms of HGT (e.g., conjugation, transformation, and transduction; Thomas and Nielsen, 2005) that involve cell-to-cell contact or access to free DNA in the environment. In addition, we found that Gram-negative bacteria
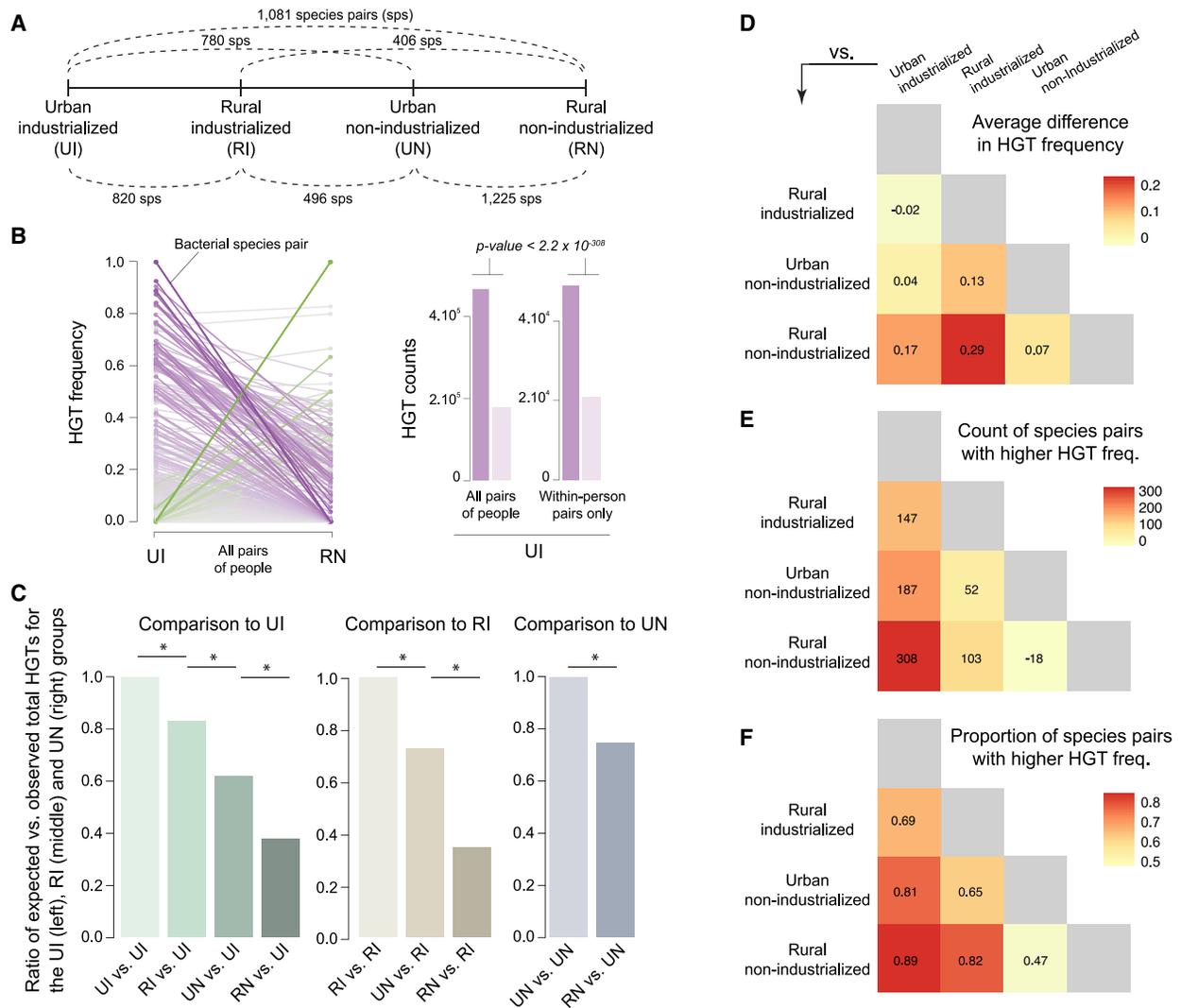
Figure 4. Higher HGT frequency in the gut microbiomes of industrialized populations

(A) Lifestyle pairs used to measure the effect of industrialization and urbanization on HGT frequencies. See Table S1 for population groupings.

(B) Comparison of HGT frequencies for pairs of species sampled in both the UI and RN groups, averaged across all pairs of people. Each line represents a species pair. The order in which lines are displayed is at random. Differences in HGT frequency between the two groups are colored along a gradient from gray (no difference) to purple (higher HGT frequency in the UI group) or from gray to green (higher HGT in the RN group). Barplots show the observed total HGT found in the UI group compared to their expected value (see STAR Methods). The number of species pairs and genomes for each comparison and category are listed in Table S6.

(C) HGT counts compared across all lifestyle pairs. For lifestyle pairs involving the UI group (left barplot), we computed the observed total HGTs of bacterial species pairs sampled in both groups and generated an expected total HGT value for the UI group. The ratios of observed versus expected HGT counts for the UI group were computed for each lifestyle pair and are shown relative to the UI group. We used the same approach for lifestyle pairs involving the RI group (middle barplot) and the UN group (right barplot). See Figure S5C for the comparison of all raw HGT counts. *p value $< 2.2 \times 10^{-308}$.

(D) Heatmap of the average difference in HGT frequency across all lifestyle pairs. Columns are compared against rows, with positive differences indicating higher HGT frequencies in lifestyles described in columns.

(E) Heatmap of the difference in the absolute count of bacterial species pairs with higher HGT frequency, across all lifestyle pairs. Columns are compared against rows, with positive counts indicating a higher number of bacterial species pairs with higher HGT frequency in lifestyles described in columns. Species pairs with no HGT observed in neither category of lifestyle pairs were excluded from the counts.

(F) Heatmap of the proportion of bacterial species pairs with higher HGT frequency, across all lifestyle pairs. Columns are compared against rows, with proportions higher than 50% indicating a higher proportion of bacterial species pairs with higher HGT frequency in lifestyles described in columns. Species pairs with no HGT observed in neither category of lifestyle pairs were excluded from the counts.

A

B
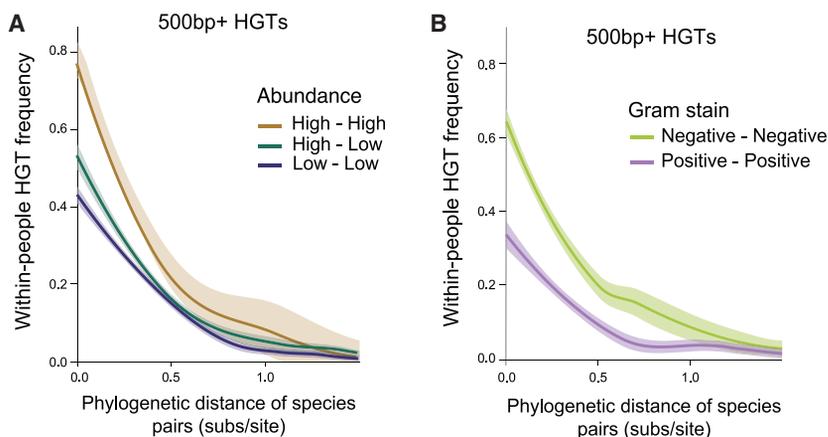
Figure 5. Highly abundant bacteria and Gram-negative bacteria are associated with higher rates of HGT
(A) Contribution of bacterial species abundance to HGT frequency, considering different species abundance bins (LOESS regression; see STAR Methods).
(B) Contribution of cell wall architecture to HGT frequency (LOESS regression; see STAR Methods).

engage more frequently in HGTs than Gram-positive bacteria (N = 10,104; OR for Gram-negative bacteria = 9.2; 95% CI = 6.6–12.8; LRT, χ^2 = 166.3, p value = 4.7 × 10^{-38}; Figure 5B). This intriguing result motivates further investigation to understand the mechanisms driving increased rates of HGT between intestinal Gram-negative bacteria.

Functions of recent HGTs reflect host lifestyle

We reasoned that if HGT can occur rapidly in response to changes in host lifestyle, then the type of genes being transferred should reflect the selective pressures associated with different populations (Brito et al., 2016). We first compared the profile of HGTs across broadly defined functional categories using species pairs found across different lifestyles. We found significant differences in HGT functions, with the rural nonindustrialized cohort having the most different profile compared to other lifestyles (Figure 6; χ^2 goodness-of-fit test, p values < 0.001).

We then focused on genes involved in key functions that likely differ across populations, such as antibiotic resistance, CAZyme, and virulence genes. We also looked at genes involved in the function of mobile genetic systems (such as phages, plasmids, and transposons). We found that gut bacteria in industrialized populations tend to have higher rates of gene exchange for genes involved in plasmids and transposons (Figure S6B; two-proportions Z-tests, corrected p values < 0.001). This finding is consistent with the elevated rates of HGT that we observed in the gut microbiomes of these individuals (Figure 4). In almost all comparisons, nonindustrialized cohorts, who generally consume larger amounts of nondigestible fiber (Makki et al., 2018; Smits et al., 2017), harbored gut bacteria that exchanged CAZyme genes at higher frequencies than individuals living in industrialized and/or urban regions (Figure 6). High transfer rates of antibiotic resistance genes were also found in the gut microbiomes of both urban and rural nonindustrialized populations, which correlates with the higher environmental prevalence of ARGs in low- and middle-income countries (Hendriksen et al., 2019; Pehrsson et al., 2016). This is further consistent with studies showing that antimicrobial resistance is increasing in livestock from low- and middle-income regions (Van Boeckel et al., 2019).

We found that the Datoga, Tanzanian pastoralists who primarily raise cattle and consume high levels of meat and dairy products from their animals, had the highest levels of ARG transfers (Figure S6C). Like other pastoral farmers in northern Tanzania, they frequently administer antibiotics to their herds (Caudell et al., 2017; Sieff, 1999). Our results suggest that these recent agricultural practices rapidly altered the fitness landscape in the guts of the Datoga people and have impacted the patterns of gene transfers within their microbiomes. As the use of commercial antimicrobials is now widespread among pastoralist populations in developing countries, similar effects may occur in many populations worldwide, with broader impact on the spread of antimicrobial resistance outside the clinic.

DISCUSSION

This article reports a large-scale genomic investigation of the effects of industrialization and urbanization on HGTs in the human gut microbiome. Taken together, our results suggest that HGT occurs frequently within individual gut microbiomes and with higher frequencies in industrialized populations. These results indicate that transitioning to industrialized (and urban) lifestyles resulted in an increase in gene transfers within the gut microbiome. One possible explanation for this observation could be that increased population density and/or perturbations in the gut ecosystem associated with the consumption of processed foods and increased sanitation promote more frequent gene exchange in the gut microbiome. The overall elevated frequency of HGTs in industrialized microbiomes could also indirectly result from the shifts in microbiome composition that occur when transitioning to industrialized lifestyles (Vangay et al., 2018), resulting in new assortments of species that frequently exchange genes. However, our analyses captured an intrinsic response of bacterial genomes to industrialization, as our HGT estimates were calculated for pairs of species that were present across different lifestyles, in all pairs of population groups under comparison.

Microbiome perturbations that occur during adaptation to industrialization are hypothesized to contribute both to the establishment of low-grade chronic intestinal inflammation in healthy individuals and to the higher incidence of inflammation-associated diseases of the industrialized world, such as inflammatory bowel disease (Sonnenburg and Sonnenburg, 2019b). Inflamed environments drive changes in species composition by favoring the bloom of oxygen-tolerant and pathogenic species that are particularly prone to engage in HGT (Zeng et al., 2017),
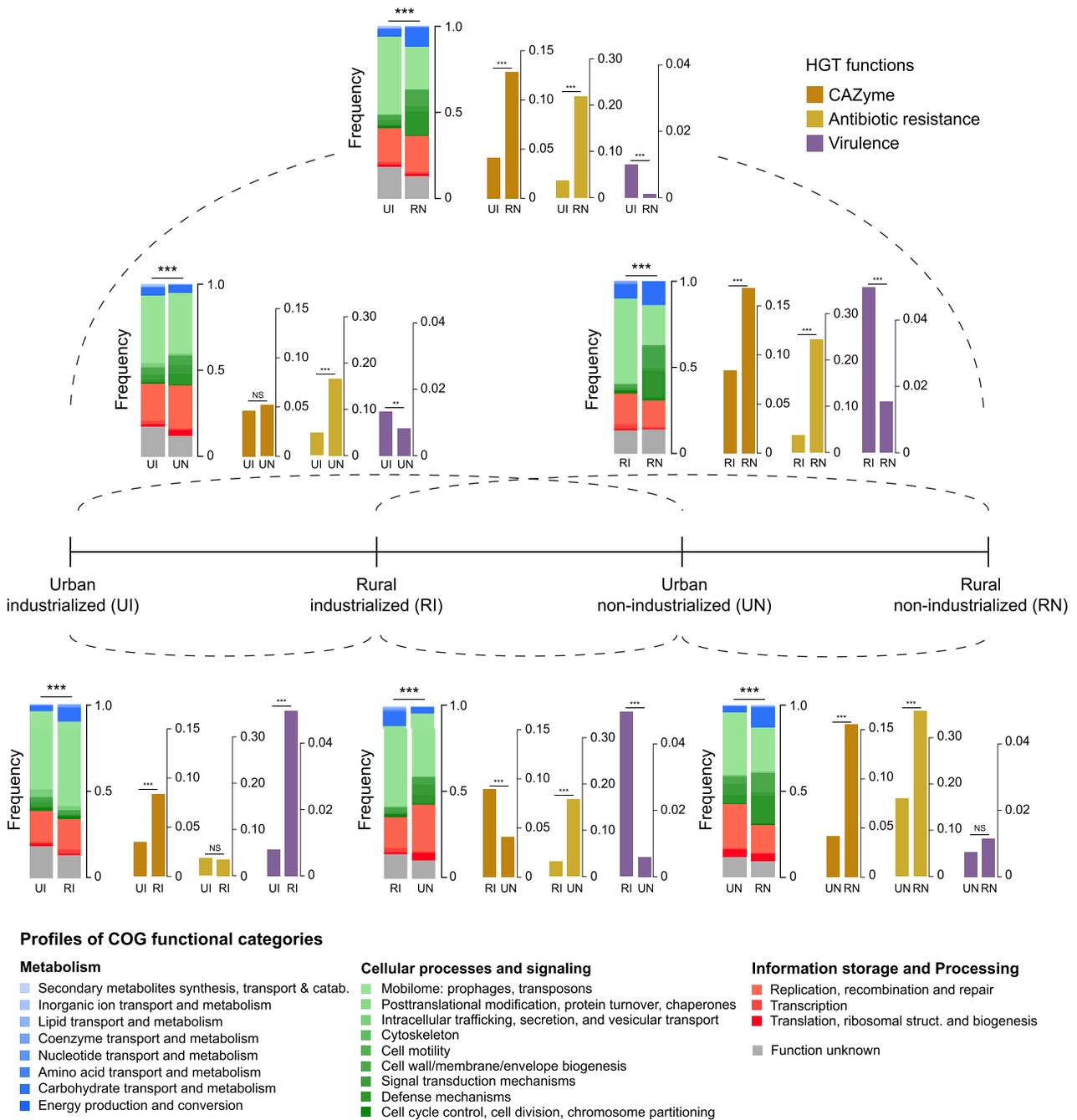
Figure 6. Functions of recently transferred genes are associated with host lifestyle

Functional profiles of transferred genes were compared across our gradient of industrialization and urbanization. COG profiles were compared using χ^2 goodness-of-fit tests (***p values < 0.001); HGT frequencies for ARG, CAZyme, and virulence genes were compared for all lifestyle pairs using two-proportion Z-tests followed by Bonferroni correction for multiple tests (**p values < 0.01; ***p values < 0.001). For a given cohort pair of different lifestyles, functions were averaged across all pairs of individuals in each cohort. In addition, for any given cohort comparison, frequencies of HGT functions were calculated using only species pairs that were sampled in both cohorts. Because sets of co-sampled species change across pairwise cohort comparisons, the functional HGT profile of a given cohort differs slightly from one cohort pair to another. However, these differences are nonsignificant (Levene's test for homogeneity of variance, p value = 0.17; see Figure S6A), suggesting that our functional HGT profiles are not biased by differences in species sampling.

such as Enterobacteriaceae. In a mouse colitis model, *Salmonella enterica* and *Escherichia coli* were previously shown to bloom and to engage in HGT (Stecher et al., 2012). Further investigations are needed to illuminate how inflammation could drive the increase in HGT in the industrialized microbiome.

Numerous studies have investigated how changes in diet and clinical practices, such as fecal microbiota transplants (Li et al., 2016; Smillie et al., 2018), impact the composition of the gut microbiome, but inferring mechanistic understanding from compositional changes is difficult. Our study reveals that HGT within the gut microbiome reflects the unique selective pressures of each human host. Thus, HGT patterns can be used to identify selective forces acting within each individual and thereby to gain a more mechanistic understanding of these events. Our results also show that whole-genome sequencing data provide information on individual microbiome function at a level of precision that popular approaches, such as 16S amplicon and metagenomic sequencing, cannot achieve. Finally, the high rate of HGT in the human gut may be a recent development in response to the industrialized lifestyle, accompanied by changes in the function of genes being exchanged. Further work is needed to appreciate the consequences of these shifts in HGT frequency and function for human health.

Limitations of study

Our study has limitations. First, our sampling design did not allow us to quantify rates of gene acquisition in nonindustrialized individuals. Many nonindustrialized populations have seasonal variations in diet and social activities, which are reflected in seasonal variations in microbiome compositions (Smits et al., 2017). It is likely that variations in these environmental factors also impose varying selective pressures on gut bacteria. Investigating such effects on the frequency and patterns of HGTs would greatly contribute to our understanding of how the gut microbiome responds to lifestyle. Second, we did not examine the mechanisms by which lifestyle-associated factors may drive increased HGT in the gut microbiome of industrialized populations.

STAR★METHODS

Detailed methods are provided in the online version of this paper and include the following:

- KEY RESOURCES TABLE
- RESOURCE AVAILABILITY
  - ○ Lead contact
  - ○ Materials availability
  - ○ Data and code availability
- EXPERIMENTAL MODEL AND SUBJECT DETAILS
  - ○ Study cohorts
  - ○ Sample collection
  - ○ Isolate genome dataset
- METHOD DETAILS
  - ○ DNA extraction, library construction and Illumina sequencing for shotgun metagenomics
  - ○ Culturing and isolation of bacterial isolates
  - ○ DNA extraction, library construction and Illumina sequencing of whole genomes

- ○ Draft assembly and annotation of whole genome sequences
- ○ Assessing assembly quality
- ○ Clustering genomes into species
- ○ Comparison to the UHGG database
- ○ Phylogenetic reconstructions
- ○ Detection and age of HGTs
- ○ Calculating HGT counts and frequencies
- ○ Simulation of HGT transmission across host generations
- ○ Calculating gene gain and loss rates in the pangenome
- ○ Analysis of metagenomic data
- ○ Measuring the abundance of isolate genomes
- ○ Assigning Gram stain to bacterial species
- ○ Annotating transferred genes
- QUANTIFICATION AND STATISTICAL ANALYSES
  - ○ Comparing HGT frequencies and counts
  - ○ Calculating the frequency of transferred genes within bacterial populations
  - ○ Controlling for the effect of phylogeny on within-person versus between-people HGT
  - ○ Controlling for the effect of *in vitro* culturing
  - ○ Permutation test to compare HGTs from populations with different lifestyles
  - ○ Measuring the effect of bacterial phylogeny, abundance and cell-wall architecture on HGT
  - ○ Comparing functional profiles of HGTs
  - ○ LOESS regressions

AUTHOR CONTRIBUTIONS

M.G., M.P., and E.J.A. designed this study. M.G., M.P., A.S., K.M., R.E.S., R.J.X., and E.J.A. founded the GMbC project under which field collections occurred. M.G. and M.P. managed field administrative work and performed the collection of data and samples. A.S., M.N., J.H., S.M.G., L.S., A. Froment, R.S.M., A. Fezeu, V.A.J., S.L., F.E.T., C.G., L.T.T.N., D.I., B.J.S., J.L., L.R., P.P.K., T.V., S.S., A.M., M.D.-R., Y.A.N., AA.-N, A.D., Y.A.A., K.A.V., S.O.A., M.Y.A., L.R.R., A.P., and C.A.O. provided local support, and contributed to

the field administrative work and the collection of data and samples. M.P. performed bacteria culturing, DNA extraction from isolates, and library preparation for whole-genome sequencing. M.P. performed DNA extraction from stool samples and library preparation for metagenomics sequencing. M.G. performed computational work and data analyses. M.G. and S.M.K. performed functional annotations on transferred genes. M.G., M.P., and E.J.A. analyzed the results. M.G., M.P., and E.J.A. wrote the manuscript, which was improved by K.M. and all other authors.

DECLARATION OF INTERESTS

R.J.X. is a consultant to Novartis and Nestle. E.J.A. is a co-founder and shareholder of Finch Therapeutics, a company that specializes in microbiome-targeted therapeutics.

INCLUSION AND DIVERSITY

We worked to ensure gender balance in the recruitment of human subjects. We worked to ensure ethnic or other types of diversity in the recruitment of human subjects. We worked to ensure that the study questionnaires were prepared in an inclusive way. One or more of the authors of this paper self-identifies as an underrepresented ethnic minority in science. One or more of the authors of this paper self-identifies as a member of the LGBTQ+ community. The author list of this paper includes contributors from the location where the research was conducted who participated in the data collection, design, analysis, and/or interpretation of the work.

REFERENCES

Almeida, A., Nayfach, S., Boland, M., Strozzi, F., Beracochea, M., Shi, Z.J., Pollard, K.S., Sakharova, E., Parks, D.H., Hugenholtz, P., et al. (2021). A unified catalog of 204,938 reference genomes from the human gut microbiome. Nat. Biotechnol. 39, 105–114.

Bankevich, A., Nurk, S., Antipov, D., Gurevich, A.A., Dvorkin, M., Kulikov, A.S., Lesin, V.M., Nikolenko, S.I., Pham, S., Prjibelski, A.D., et al. (2012). SPAdes: a new genome assembly algorithm and its applications to single-cell sequencing. J. Comput. Biol. 19, 455–477.

Bates, D., Mächler, M., Bolker, B., and Walker, S. (2015). Fitting Linear Mixed-Effects Models Usinglme4. J. Stat. Softw. 67, 1–48.

Boetzer, M., Henkel, C.V., Jansen, H.J., Butler, D., and Pirovano, W. (2011). Scaffolding pre-assembled contigs using SSPACE. Bioinformatics 27, 578–579.

Bolger, A.M., Lohse, M., and Usadel, B. (2014). Trimmomatic: a flexible trimmer for Illumina sequence data. Bioinformatics 30, 2114–2120.

Brewster, R., Tamburini, F.B., Asiimwe, E., Oduaran, O., Hazelhurst, S., and Bhatt, A.S. (2019). Surveying Gut Microbiome Research in Africans: Toward Improved Diversity and Representation. Trends Microbiol. 27, 824–835.

Brito, I.L., Yilmaz, S., Huang, K., Xu, L., Jupiter, S.D., Jenkins, A.P., Naisilisili, W., Tamminen, M., Smillie, C.S., Wortman, J.R., et al. (2016). Mobile genes in the human microbiome are structured from global to individual scales. Nature 535, 435–439.

Browne, H.P., Forster, S.C., Anonye, B.O., Kumar, N., Neville, B.A., Stares, M.D., Goulding, D., and Lawley, T.D. (2016). Culturing of 'unculturable' human microbiota reveals novel taxa and extensive sporulation. Nature 533, 543–546.

Buchfink, B., Xie, C., and Huson, D.H. (2015). Fast and sensitive protein alignment using DIAMOND. Nat. Methods 12, 59–60.

Camacho, C., Coulouris, G., Avagyan, V., Ma, N., Papadopoulos, J., Bealer, K., and Madden, T.L. (2009). BLAST+: architecture and applications. BMC Bioinformatics 10, 421.

Caudell, M.A., Quinlan, M.B., Subbiah, M., Call, D.R., Roulette, C.J., Roulette, J.W., Roth, A., Matthews, L., and Quinlan, R.J. (2017). Antimicrobial Use and Veterinary Care among Agro-Pastoralists in Northern Tanzania. PLoS ONE 12, e0170328.

Coyne, M.J., Zitomersky, N.L., McGuire, A.M., Earl, A.M., and Comstock, L.E. (2014). Evidence of extensive DNA transfer between bacteroidales species within the human gut. MBio 5, e01305–e01314.

Criscuolo, A., and Gribaldo, S. (2010). BMGE (Block Mapping and Gathering with Entropy): a new software for selection of phylogenetic informative regions from multiple sequence alignments. BMC Evol. Biol. 10, 210.

Croucher, N.J., Page, A.J., Connor, T.R., Delaney, A.J., Keane, J.A., Bentley, S.D., Parkhill, J., and Harris, S.R. (2015). Rapid phylogenetic analysis of large samples of recombinant bacterial whole genome sequences using Gubbins. Nucleic Acids Res. 43, e15.

de Vries, J. (1994). The Industrial Revolution and the Industrious Revolution. J. Econ. Hist. 54, 249–270.

Didelot, X., Walker, A.S., Peto, T.E., Crook, D.W., and Wilson, D.J. (2016). Within-host evolution of bacterial pathogens. Nat. Rev. Microbiol. 14, 150–162.

Drake, J.W. (1991). A constant rate of spontaneous mutation in DNA-based microbes. Proc. Natl. Acad. Sci. USA 88, 7160–7164.

Duchêne, S., Holt, K.E., Weill, F.-X., Le Hello, S., Hawkey, J., Edwards, D.J., Fourment, M., and Holmes, E.C. (2016). Genome-scale rates of evolutionary change in bacteria. Microb. Genom. 2, e000094.

Faith, J.J., Guruge, J.L., Charbonneau, M., Subramanian, S., Seedorf, H., Goodman, A.L., Clemente, J.C., Knight, R., Heath, A.C., Leibel, R.L., et al. (2013). The long-term stability of the human gut microbiota. Science 341, 1237439.

Ferretti, P., Pasolli, E., Tett, A., Asnicar, F., Gorfer, V., Fedi, S., Armanini, F., Truong, D.T., Manara, S., Zolfo, M., et al. (2018). Mother-to-Infant Microbial Transmission from Different Body Sites Shapes the Developing Infant Gut Microbiome. Cell Host Microbe 24, 133–145.e5.

Forsberg, K.J., Reyes, A., Wang, B., Selleck, E.M., Sommer, M.O.A., and Dantas, G. (2012). The shared antibiotic resistome of soil bacteria and human pathogens. Science 337, 1107–1111.

Forster, S.C., Kumar, N., Anonye, B.O., Almeida, A., Viciani, E., Stares, M.D., Dunn, M., Mkandawire, T.T., Zhu, A., Shao, Y., et al. (2019). A human gut bacterial genome and culture collection for improved metagenomic analyses. Nat. Biotechnol. 37, 186–192.

Garrity, G. (2005). Bergey's Manual of Systematic Bacteriology: Volume 2: The Proteobacteria (Springer).

Garud, N.R., Good, B.H., Hallatschek, O., and Pollard, K.S. (2019). Evolutionary dynamics of bacteria in the gut microbiome within and across hosts. PLoS Biol. 17, e3000102.

Gibbons, S.M., Kearney, S.M., Smillie, C.S., and Alm, E.J. (2017). Two dynamic regimes in the human gut microbiome. PLoS Comput. Biol. 13, e1005364.

Gibson, M.K., Forsberg, K.J., and Dantas, G. (2015). Improved annotation of antibiotic resistance determinants reveals microbial resistomes cluster by ecology. ISME J. 9, 207–216.

Goodman, A.L., Kallstrom, G., Faith, J.J., Reyes, A., Moore, A., Dantas, G., and Gordon, J.I. (2011). Extensive personal human gut microbiota culture collections characterized and manipulated in gnotobiotic mice. Proc. Natl. Acad. Sci. USA 108, 6252–6257.

Gouy, M., Guindon, S., and Gascuel, O. (2010). SeaView version 4: A multiplatform graphical user interface for sequence alignment and phylogenetic tree building. Mol. Biol. Evol. 27, 221–224.

Hansen, M.E.B., Rubel, M.A., Bailey, A.G., Ranciaro, A., Thompson, S.R., Campbell, M.C., Beggs, W., Dave, J.R., Mokone, G.G., Mpoloka, S.W., et al. (2019). Population structure of human gut bacteria in a diverse cohort from rural Tanzania and Botswana. Genome Biol. 20, 16.

Hehemann, J.-H., Correc, G., Barbeyron, T., Helbert, W., Czjzek, M., and Michel, G. (2010). Transfer of carbohydrate-active enzymes from marine bacteria to Japanese gut microbiota. Nature *464*, 908–912.

Hendriksen, R.S., Munk, P., Njage, P., van Bunnik, B., McNally, L., Lukjancenko, O., Röder, T., Nieuwenhuijse, D., Pedersen, S.K., Kjeldgaard, J., et al.; Global Sewage Surveillance project consortium (2019). Global monitoring of antimicrobial resistance based on metagenomics analyses of urban sewage. Nat. Commun. *10*, 1124.

Huerta-Cepas, J., Forslund, K., Coelho, L.P., Szklarczyk, D., Jensen, L.J., von Mering, C., and Bork, P. (2017). Fast Genome-Wide Functional Annotation through Orthology Assignment by eggNOG-Mapper. Mol. Biol. Evol. *34*, 2115–2122.

Hyatt, D., Chen, G.-L., Locascio, P.F., Land, M.L., Larimer, F.W., and Hauser, L.J. (2010). Prodigal: prokaryotic gene recognition and translation initiation site identification. BMC Bioinformatics *11*, 119.

Jauffrit, F., Penel, S., Delmotte, S., Rey, C., de Vienne, D.M., Gouy, M., Charrier, J.-P., Flandrois, J.-P., and Brochier-Armanet, C. (2016). RiboDB Database: A Comprehensive Resource for Prokaryotic Systematics. Mol. Biol. Evol. *33*, 2170–2172.

Jones, P., Binns, D., Chang, H.-Y., Fraser, M., Li, W., McAnulla, C., McWilliam, H., Maslen, J., Mitchell, A., Nuka, G., et al. (2014). InterProScan 5: genome-scale protein function classification. Bioinformatics *30*, 1236–1240.

Konstantinidis, K.T., and Tiedje, J.M. (2005). Genomic insights that advance the species definition for prokaryotes. Proc. Natl. Acad. Sci. USA *102*, 2567–2572.

Krieg, N.R., Ludwig, W., Whitman, W.B., Hedlund, B.P., Paster, B.J., Staley, J.T., Ward, N., and Brown, D. (2011). Bergey's Manual of Systematic Bacteriology: Volume 4: The Bacteroidetes, Spirochaetes, Tenericutes (Mollicutes), Acidobacteria, Fibrobacteres, Fusobacteria, Dictyoglomi, Gemmatimonadetes, Lentisphaerae, Verrucomicrobia, Chlamydiae, and Planctomycetes (Springer Science & Business Media).

Li, H., and Durbin, R. (2009). Fast and accurate short read alignment with Burrows-Wheeler transform. Bioinformatics *25*, 1754–1760.

Li, S.S., Zhu, A., Benes, V., Costea, P.I., Hercog, R., Hildebrand, F., Huerta-Cepas, J., Nieuwdorp, M., Salojärvi, J., Voigt, A.Y., et al. (2016). Durable coexistence of donor and recipient strains after fecal microbiota transplantation. Science *352*, 586–589.

Lopatkin, A.J., Meredith, H.R., Srimani, J.K., Pfeiffer, C., Durrett, R., and You, L. (2017). Persistence and reversal of plasmid-mediated antibiotic resistance. Nat. Commun. *8*, 1689.

Lu, J., Breitwieser, F.P., Thielen, P., and Salzberg, S.L. (2017). Bracken: estimating species abundance in metagenomics data. PeerJ Comput. Sci. *3*, e104.

Makki, K., Deehan, E.C., Walter, J., and Bäckhed, F. (2018). The Impact of Dietary Fiber on Gut Microbiota in Host Health and Disease. Cell Host Microbe *23*, 705–715.

Martin, M. (2011). Cutadapt removes adapter sequences from high-throughput sequencing reads. EMBnet. J. *17*, 10.

McDonald, D., Hyde, E., Debelius, J.W., Morton, J.T., Gonzalez, A., Ackermann, G., Aksenov, A.A., Behsaz, B., Brennan, C., Chen, Y., et al.; American Gut Consortium (2018). American Gut: an Open Platform for Citizen Science Microbiome Research. mSystems *3*, e00031, e18.

Mehta, R.S., Abu-Ali, G.S., Drew, D.A., Lloyd-Price, J., Subramanian, A., Lochhead, P., Joshi, A.D., Ivey, K.L., Khalili, H., Brown, G.T., et al. (2018). Stability of the human faecal microbiome in a cohort of adult men. Nat. Microbiol. *3*, 347–355.

Mira, A., Ochman, H., and Moran, N.A. (2001). Deletional bias and the evolution of bacterial genomes. Trends Genet. *17*, 589–596.

Mistry, J., Finn, R.D., Eddy, S.R., Bateman, A., and Punta, M. (2013). Challenges in homology search: HMMER3 and convergent evolution of coiled-coil regions. Nucleic Acids Res. *41*, e121.

Modi, S.R., Lee, H.H., Spina, C.S., and Collins, J.J. (2013). Antibiotic treatment expands the resistance reservoir and ecological network of the phage metagenome. Nature *499*, 219–222.

Munck, C., Sheth, R.U., Freedberg, D.E., and Wang, H.H. (2020). Recording mobile DNA in the gut microbiota using an Escherichia coli CRISPR-Cas spacer acquisition platform. Nat. Commun. *11*, 95.

Nadalin, F., Vezzi, F., and Policriti, A. (2012). GapFiller: a de novo assembly approach to fill the gap within paired reads. BMC Bioinformatics *13* (*Suppl 14*), S8.

Nakamura, T., Yamada, K.D., Tomii, K., and Katoh, K. (2018). Parallelization of MAFFT for large-scale multiple sequence alignments. Bioinformatics *34*, 2490–2492.

NCBI Resource Coordinators (2016). Database resources of the National Center for Biotechnology Information. Nucleic Acids Res. *44* (D1), D7–D19.

Oksanen, J., Blanchet, F.G., Friendly, M., Kindt, R., Legendre, P., McGlinn, D., Minchin, P.R., O'Hara, R.B., Simpson, G.L., Solymos, P., et al. (2019). vegan: Community Ecology Package. https://cran.r-project.org/web/packages/vegan/index.html.

Ondov, B.D., Treangen, T.J., Melsted, P., Mallonee, A.B., Bergman, N.H., Koren, S., and Phillippy, A.M. (2016). Mash: fast genome and metagenome distance estimation using MinHash. Genome Biol. *17*, 132.

Page, A.J., Cummins, C.A., Hunt, M., Wong, V.K., Reuter, S., Holden, M.T.G., Fookes, M., Falush, D., Keane, J.A., and Parkhill, J. (2015). Roary: rapid large-scale prokaryote pan genome analysis. Bioinformatics *31*, 3691–3693.

Page, A.J., Taylor, B., Delaney, A.J., Soares, J., Seemann, T., Keane, J.A., and Harris, S.R. (2016). *SNP-sites*: rapid efficient extraction of SNPs from multi-FASTA alignments. Microb. Genom. *2*, e000056.

Parks, D.H., Imelfort, M., Skennerton, C.T., Hugenholtz, P., and Tyson, G.W. (2015). CheckM: assessing the quality of microbial genomes recovered from isolates, single cells, and metagenomes. Genome Res. *25*, 1043–1055.

Pasolli, E., Asnicar, F., Manara, S., Zolfo, M., Karcher, N., Armanini, F., Beghini, F., Manghi, P., Tett, A., Ghensi, P., et al. (2019). Extensive Unexplored Human Microbiome Diversity Revealed by Over 150,000 Genomes from Metagenomes Spanning Age, Geography, and Lifestyle. Cell *176*, 649–662.e20.

Pehrsson, E.C., Tsukayama, P., Patel, S., Mejía-Bautista, M., Sosa-Soto, G., Navarrete, K.M., Calderon, M., Cabrera, L., Hoyos-Arango, W., Bertoli, M.T., et al. (2016). Interconnected microbiomes and resistomes in low-income human habitats. Nature *533*, 212–216.

Poyet, M., Groussin, M., Gibbons, S.M., Avila-Pacheco, J., Jiang, X., Kearney, S.M., Perrotta, A.R., Berdy, B., Zhao, S., Lieberman, T.D., et al. (2019). A library of human gut bacterial isolates paired with longitudinal multiomics data enables mechanistic microbiome research. Nat. Med. *25*, 1442–1452.

Price, M.N., Dehal, P.S., and Arkin, A.P. (2010). FastTree 2–approximately maximum-likelihood trees for large alignments. PLoS ONE *5*, e9490.

Rognes, T., Flouri, T., Nichols, B., Quince, C., and Mahé, F. (2016). VSEARCH: a versatile open source tool for metagenomics. PeerJ *4*, e2584.

Schnorr, S.L., Candela, M., Rampelli, S., Centanni, M., Consolandi, C., Basaglia, G., Turroni, S., Biagi, E., Peano, C., Severgnini, M., et al. (2014). Gut microbiome of the Hadza hunter-gatherers. Nat. Commun. *5*, 3654.

SEDAC Population Estimation Service (2015). https://sedac.ciesin.columbia.edu/mapping/popest/pes-v3/.

Seemann, T. (2014). Prokka: rapid prokaryotic genome annotation. Bioinformatics *30*, 2068–2069.

Sieff, D.F. (1999). The effects of wealth on livestock dynamics among the Datoga pastoralists of Tanzania. Agric. Syst. *59*, 1–25.

Smillie, C.S., Smith, M.B., Friedman, J., Cordero, O.X., David, L.A., and Alm, E.J. (2011). Ecology drives a global network of gene exchange connecting the human microbiome. Nature *480*, 241–244.

Smillie, C.S., Sauk, J., Gevers, D., Friedman, J., Sung, J., Youngster, I., Hohmann, E.L., Staley, C., Khoruts, A., Sadowsky, M.J., et al. (2018). Strain Tracking Reveals the Determinants of Bacterial Engraftment in the Human

Gut Following Fecal Microbiota Transplantation. Cell Host Microbe *23*, 229–240.e5.

Smits, S.A., Leach, J., Sonnenburg, E.D., Gonzalez, C.G., Lichtman, J.S., Reid, G., Knight, R., Manjurano, A., Changalucha, J., Elias, J.E., et al. (2017). Seasonal cycling in the gut microbiome of the Hadza hunter-gatherers of Tanzania. Science *357*, 802–806.

Snipen, L., and Liland, K.H. (2015). micropan: an R-package for microbial pangenomics. BMC Bioinformatics *16*, 79.

Sonnenburg, E.D., and Sonnenburg, J.L. (2019a). The ancestral and industrialized gut microbiota and implications for human health. Nat. Rev. Microbiol. *17*, 383–390.

Sonnenburg, J.L., and Sonnenburg, E.D. (2019b). Vulnerability of the industrialized microbiota. Science *366*, eaaw9255.

Stecher, B., Denzler, R., Maier, L., Bernet, F., Sanders, M.J., Pickard, D.J., Barthel, M., Westendorf, A.M., Krogfelt, K.A., Walker, A.W., et al. (2012). Gut inflammation can boost horizontal gene transfer between pathogenic and commensal Enterobacteriaceae. Proc. Natl. Acad. Sci. USA *109*, 1269–1274.

Thomas, C.M., and Nielsen, K.M. (2005). Mechanisms of, and barriers to, horizontal gene transfer between bacteria. Nat. Rev. Microbiol. *3*, 711–721.

United Nations Development Program (2020). http://www.hdr.undp.org/en/data.

Van Boeckel, T.P., Pires, J., Silvester, R., Zhao, C., Song, J., Criscuolo, N.G., Gilbert, M., Bonhoeffer, S., and Laxminarayan, R. (2019). Global trends in antimicrobial resistance in animals in low- and middle-income countries. Science *365*, eaaw1944.

Vangay, P., Johnson, A.J., Ward, T.L., Al-Ghalith, G.A., Shields-Cutler, R.R., Hillmann, B.M., Lucas, S.K., Beura, L.K., Thompson, E.A., Till, L.M., et al. (2018). US Immigration Westernizes the Human Gut Microbiome. Cell *175*, 962–972.e10.

Wood, D.E., Lu, J., and Langmead, B. (2019). Improved metagenomic analysis with Kraken 2. Genome Biol. *20*, 257.

Xu, H., Luo, X., Qian, J., Pang, X., Song, J., Qian, G., Chen, J., and Chen, S. (2012). FastUniq: a fast de novo duplicates removal tool for paired short reads. PLoS ONE *7*, e52249.

Yaffe, E., and Relman, D.A. (2020). Tracking microbial evolution in the human gut using Hi-C reveals extensive horizontal gene transfer, persistence and adaptation. Nat. Microbiol. *5*, 343–353.

Yatsunenko, T., Rey, F.E., Manary, M.J., Trehan, I., Dominguez-Bello, M.G., Contreras, M., Magris, M., Hidalgo, G., Baldassano, R.N., Anokhin, A.P., et al. (2012). Human gut microbiome viewed across age and geography. Nature *486*, 222–227.

Yin, Y., Mao, X., Yang, J., Chen, X., Mao, F., and Xu, Y. (2012). dbCAN: a web resource for automated carbohydrate-active enzyme annotation. Nucleic Acids Res. *40*, W445-51.

Zeileis, A., and Hothorn, T. (2002). Diagnostic Checking in Regression Relationships. R News *2*, 7–10.

Zeng, M.Y., Inohara, N., and Nuñez, G. (2017). Mechanisms of inflammation-driven bacterial dysbiosis in the gut. Mucosal Immunol. *10*, 18–26.

Zhao, S., Lieberman, T.D., Poyet, M., Kauffman, K.M., Gibbons, S.M., Groussin, M., Xavier, R.J., and Alm, E.J. (2019). Adaptive Evolution within Gut Microbiomes of Healthy People. Cell Host Microbe *25*, 656–667.e8.

Zlitni, S., Bishara, A., Moss, E.L., Tkachenko, E., Kang, J.B., Culver, R.N., Andermann, T.M., Weng, Z., Wood, C., Handy, C., et al. (2020). Strain-resolved microbiome sequencing reveals mobile elements that drive bacterial competition on a clinical timescale. Genome Med. *12*, 50.

Zou, Y., Xue, W., Luo, G., Deng, Z., Qin, P., Guo, R., Sun, H., Xia, Y., Liang, S., Dai, Y., et al. (2019). 1,520 reference genomes from cultivated human gut bacteria enable functional microbiome analyses. Nat. Biotechnol. *37*, 179–185.

STAR★METHODS

KEY RESOURCES TABLE

REAGENT or RESOURCE	SOURCE	IDENTIFIER
Bacterial strains		
From GMbC individuals	This paper, see Table S2	dbGaP Study ID: 38715, Accession: phs002235.v1.p1
From USA individuals of the Boston area	Poyet et al., 2019	NCBI, BioProject PRJNA544527
Critical commercial assays		
DNeasy PowerSoil Kit	QIAGEN	Cat No./ID: 12955-4
DNeasy UltraClean 96 Microbial Kit	QIAGEN	Cat No./ID: 10196-4
Nextera® DNA Sample Preparation Kit	Illumina	Cat No./ID: FC-121-1031
Deposited data		
Metagenomes and isolate genomes from GMbC individuals	This paper	dbGaP Study ID: 38715, Accession: phs002235.v1.p1
Metagenomes and isolate genomes from USA individuals	Poyet et al., 2019	NCBI, BioProject PRJNA544527
Software and algorithms		
cutadapt (version 1.12)	Martin, 2011	https://cutadapt.readthedocs.io/en/stable/
Trimmomatic (version 0.36)	Bolger et al., 2014	http://www.usadellab.org/cms/?page=trimmomatic
SPAdes (version 0.3.9.1)	Bankevich et al., 2012	https://github.com/ablab/spades
SSPACE (version 3.0)	Boetzer et al., 2011	https://github.com/nsoranzo/sspace_basic
GapFiller (version 1-10)	Nadalin et al., 2012	https://sourceforge.net/projects/gapfiller/
BBmap (version 37.68)	BBMap – Bushnell B. – https://sourceforge.net/projects/bbmap/	https://jgi.doe.gov/data-and-tools/bbtools/
Prokka (version 1.12)	Seemann, 2014	https://github.com/tseemann/prokka
CheckM (version 1.0.7)	Parks et al., 2015	https://github.com/Ecogenomics/CheckM/wiki
Mash (version 1.1.1)	Ondov et al., 2016	https://mash.readthedocs.io/en/latest/
micropan R package	Snipen and Liland, 2015	https://cran.r-project.org/web/packages/micropan/index.html
Diamond (version 0.8.22.84)	Buchfink et al., 2015	https://github.com/bbuchfink/diamond
Mafft (version 7.310)	Nakamura et al., 2018	https://mafft.cbrc.jp/alignment/software/
BMGE (version 1.12)	Criscuolo and Gribaldo, 2010	ftp://ftp.pasteur.fr/pub/gensoft/projects/BMGE/
Seaview (version 4.7)	Gouy et al., 2010	http://doua.prabi.fr/software/seaview
FastTree (version 2.1.10)	Price et al., 2010	http://www.microbesonline.org/fasttree/
Roary (version 3.11.2)	Page et al., 2015	https://github.com/sanger-pathogens/Roary
Gubbins (version 2.2.0)	Croucher et al., 2015	https://sanger-pathogens.github.io/gubbins/
SNP-sites (version 2.4.1)	Page et al., 2016	https://github.com/sanger-pathogens/snp-sites
Blastn (version 2.6.0)	Camacho et al., 2009	https://ftp.ncbi.nlm.nih.gov/blast/executables/blast+/LATEST/
Trim Galore (version 0.5.0)	https://www.bioinformatics.babraham.ac.uk/projects/trim_galore/	https://github.com/FelixKrueger/TrimGalore
Fastuniq (version 1.1)	Xu et al., 2012	https://sourceforge.net/projects/fastuniq/
BWA (version 0.7.13)	Li and Durbin, 2009	https://github.com/lh3/bwa
Kraken2 (version 2.0.8-beta)	Wood et al., 2019	https://github.com/DerrickWood/kraken2/wiki
Bracken (version 2.5)	Lu et al., 2017	https://github.com/jenniferlu717/Bracken
vegan R package	Oksanen et al., 2019	https://cran.r-project.org/web/packages/vegan/index.html
Prodigal (version 2.6.3)	Hyatt et al., 2010	https://github.com/hyattpd/Prodigal

(Continued on next page)

Continued

REAGENT or RESOURCE	SOURCE	IDENTIFIER
vsearch (version 2.3.4)	Rognes et al., 2016	https://github.com/torognes/vsearch
eggNOG-mapper	Huerta-Cepas et al., 2017	http://eggnog5.embl.de/
InterProScan (version 5.36-75.0)	Jones et al., 2014	https://www.ebi.ac.uk/interpro/search/sequence/
Hmmer3 (version 3.1b2)	Mistry et al., 2013	http://hmmer.org/
lme4 R package	Bates et al., 2015	https://cran.r-project.org/web/packages/lme4/index.html
lmtest R package	Zeileis and Hothorn, 2002	https://cran.r-project.org/web/packages/lmtest/index.html
Other		
NCBI Genome database	NCBI Resource Coordinators, 2016	ftp://ftp.ncbi.nlm.nih.gov/genomes/
RiboDB database	Jauffrit et al., 2016	https://umr5558-bibiserv.univ-lyon1.fr/
Resfam database	Gibson et al., 2015	http://www.dantaslab.org/resfams
dbCAN database	Yin et al., 2012	http://bcb.unl.edu/dbCAN/

RESOURCE AVAILABILITY

Lead contact
Further information and requests for resources and reagents should be directed to and will be fulfilled by the Lead Contact, Eric J Alm.

Materials availability
Bacterial strains generated in this study are available upon request to the Lead Contact, Eric J Alm.

Data and code availability
Generated data (raw reads and genome assemblies for GMbC isolates and shotgun metagenomic data for GMbC individuals) are available online on the dbGaP server (Study ID: 38715; Accession: phs002235.v1.p1). Metagenomes and isolate genomes of USA individuals from the Boston area are available on the NCBI (BioProject PRJNA544527).

Scripts and command lines used to process the sequencing and genomic data are available at https://github.com/almlab/GMbC_HGTs

HGT data (genomic coordinates, species, individual host, length, functional annotations) are available on the Open Science Framework at https://osf.io/pr2fw/

EXPERIMENTAL MODEL AND SUBJECT DETAILS

Study cohorts
Stool samples from 37 healthy individuals recruited worldwide as part of the Global Microbiome Conservancy project (http://microbiomeconservancy.org) were obtained from Inuit individuals in Canadian Arctic, Sami and Finnish individuals in Finland, Beti and Baka individuals in Cameroon, Hadza and Datoga individuals in Tanzania, individuals from the North Plain Tribes in Montana (USA), Igbo and Yoruba individuals in Nigeria and Ashanti, Fante, Ga and Ahafo individuals in Ghana. Recruited individuals were not involved in prior procedures and did not consume antibiotics during the three months prior to recruitment. Written informed consent was obtained from all participants. Research & ethics approvals were obtained from the MIT IRB (protocol #1612797956), as well as in each sampled country prior to the start of sample collection, from the following local ethics committees: Chief Dull Knife College (Montana), protocol #FWA00020985; Comite National d'Ethique de la Recherche pour la Sante Humaine (Cameroon), protocol #2017/05/901/CE/CNERSH/SP; Nunavut Research Institute (Canada), protocol #0205217N-M; National Institute for Medical Research (Tanzania), protocol #NIMR/HQ/R.8a/Vol. IX/2657; Coordinating Ethics Committee of Helsinki and Uusimaa Hospital District (Finland), protocol #1527/2017; Cape Coast Teaching Hospital Ethical Review Committee (Ghana), protocol #CCTHERC/RS/EC/2016/3; Committee on Human Research, Publication and Ethics of the Komfo Anokye Teaching Hospital (Ghana), protocol #CHRPE/AP/398/18; National Health Research Ethics Committee of Nigeria (Nigeria), protocol #NHREC/01/01/2007-29/04/2018.

Samples from 11 additional USA individuals that we previously recruited in the Boston area (Poyet et al., 2019) were included in the study, providing a dataset of 48 individuals from 15 populations. Both male (54%) and female (46%) participants were recruited. The average age of participants is 33 yo (18-55 yo). We divided our cohort into four groups of different lifestyles: rural non-industrialized, urban non-industrialized, rural industrialized and urban industrialized according to two different parameters: the population density (SEDAC Population Estimation Service, 2015), and the level of industrialization based on the Human Development Index at the country level (United Nations Development Program, 2020). Table S1 contains metadata information about each subject enrolled in this study.

Sample collection

Participants produced a fecal sample in a sterile container that was immediately returned to researchers in the field. Raw stool was diluted 1:5 in 25% pre-reduced (anaerobic) glycerol solution containing acid-washed glass beads, and were immediately homogenized and aliquoted into cryogenic 2mL tubes. Stool samples aliquoted in cryoprotectant were immediately flash frozen in the field at −196C, using a cryoshipper tank. Samples were then shipped to MIT for processing, culturing and storage. Table S2 contains culturing information for each bacterial isolate cultured and analyzed in this study.

Isolate genome dataset

In this study, we sequenced the genome of 4,149 gut bacterial isolates that we cultured from the stool sample of 37 individuals. We completed our genome dataset with the 3,632 isolate genomes of the BIO-ML collection that we previously generated (Poyet et al., 2019) to generate a total set of 7,781 isolate genomes. Table S2 contains metadata for each of the 7,781 isolates, and Table S5 provides information about the genomes that were used in the longitudinal analysis.

METHOD DETAILS

DNA extraction, library construction and Illumina sequencing for shotgun metagenomics

We used the DNeasy PowerSoil Kit (QIAGEN) with manufacturers' protocols to extract microbial genomic DNA from stool samples. Genomic DNA libraries were constructed from 1.2ng of cleaned DNA using the Nextera DNA Library Preparation kit (Illumina) according to the manufacturer's recommended protocol, with reaction volumes scaled accordingly. Prior to sequencing, libraries were pooled by collecting equal quantity of each library from batches of 94 samples. Insert sizes and concentrations of each pooled library were determined using an Agilent Bioanalyzer DNA 1000 kit (Agilent Technologies). Paired-end sequencing (2x150-bp reads) was performed using an Illumina NextSeq 500 instrument (Illumina Inc) at the Broad Institute.

Culturing and isolation of bacterial isolates

To culture and isolate the 4,149 bacterial strains generated in this study, we used stool samples collected from 37 individuals across 14 human populations. To obtain an exhaustive representation of the diversity of human gut bacteria, human fecal samples were processed anaerobically at every step in a chamber, using gas monitors controlling physico-chemical conditions (5% Hydrogen, 20% Carbon dioxide, balanced with Nitrogen). Human fecal samples were diluted in pre-reduced PBS (with 0.1% L-cysteine hydrochloride hydrate). Diluted samples were then plated onto pre-reduced agar plates and incubated anaerobically at 37°C for 7 to 14 days. Both general (nonselective) and selective media were used to culture diverse groups of organisms. We used different culturing media, combined with antibiotic, acid, and ethanol treatments to isolate 4,149 bacterial strains. See Table S2 for culturing media used in this study and other metadata for each isolate. After incubation, bacteria were isolated by picking individual colonies with an inoculation loop. They were streaked onto a second pre-reduced agar plate to increase colony purity. After 2 days of incubation at 37°C, one colony was re-streaked again onto a third agar plate for 2 additional days of incubation. One colony from each individual streak was then inoculated in liquid media in a 96-well culture plate. After 2 days of anaerobic incubation at 37°C, the taxonomy of the isolate was identified using 16S rRNA gene Sanger sequencing (starting at the V4 region). We first amplified the full 16S rRNA gene by PCR (27f 5′-AGAGTTTGATCMTGGCTCAG-3′ - 1492r 5′-GGTTACCTTGTTACGACTT-3′) and then generated a ∼1kb long sequence by Sanger reaction (u515 5′-GTGCCAGCMGCCGCGGTAA-3′). All isolates are stored in −80°C freezers in a pre-reduced cryoprotectant glycerol buffer.

DNA extraction, library construction and Illumina sequencing of whole genomes

We used the DNeasy UltraClean96 MicrobioalKit (QIAGEN) kit to extract whole genome DNA from isolate colonies, following manufacturers' protocols. Genomic DNA libraries were constructed from 1.2ng of DNA using the Nextera DNA Library Preparation kit (Illumina), following the manufacturer's protocol, with reaction volumes scaled accordingly. Prior to sequencing, we pooled on average 250 samples with equal quantities of DNA. Insert size and concentration of each pooled library were determined using an Agilent Bioanalyzer DNA 1000 kit (Agilent Technologies). Paired-end (2x150bp) reads sequencing was performed using an Illumina NextSeq 500 instrument (Illumina Inc) at the Broad Institute.

Draft assembly and annotation of whole genome sequences

All parameters used to generate whole genome assemblies from 2x150bp paired-end data and used to perform downstream genomic analyses are embedded in the method descriptions below.

Briefly, reads were first demultiplexed using in-house scripts. We used cutadapt v1.12 (Martin, 2011) to remove barcodes and Illumina adapters (with parameters -a CTGTCTCTTAT -A CTGTCTCTTAT). We used Trimmomatic v0.36 (Bolger et al., 2014) for the quality filtering of data (with parameters PE -phred33 LEADING:3 TRAILING:3 SLIDINGWINDOW:5:20 MINLEN:50). Reads were assembled *de novo* into contigs using SPAdes v.3.9.1 (Bankevich et al., 2012) (with parameter–careful). To iteratively improve genome assemblies, we used SSPACE v3.0 (Boetzer et al., 2011) and GapFiller v1-10 (Nadalin et al., 2012) to scaffold contigs and to fill sequence gaps (with default parameters). Scaffolds smaller than 1kb were removed from genome assemblies. We aligned all reads back to the assembly to compute genome coverage using BBmap v37.68 (https://jgi.doe.gov/data-and-tools/bbtools/) and

the covstats option (with default parameters). The final assemblies were annotated using Prokka v1.12 (Seemann, 2014) (with default parameters).

Assessing assembly quality

We measured genome assembly statistics using CheckM v1.0.7 (Parks et al., 2015) (with parameters lineage_wf–tab_table -x fna Prokka_annotations/). All summary and quality statistics can be found in Table S2. The median assembly completeness of all 7,781 genomes is 99.33%, the median contamination is 0.3%, the median scaffold N50 is 144kb, and the median coverage is 120X.

Clustering genomes into species

We used whole genomic information to group genomes into species clusters. We used an open-reference approach and computed all-against-all genomic distances using Mash (Ondov et al., 2016) (with default parameters). A Mash distance lower than 0.05 is equivalent to using an Average Nucleotide Identity higher than 95%, which is a standard threshold for delineating species (Konstantinidis and Tiedje, 2005). We used an unsupervised hierarchical clustering approach to group genomes that had Mash distances ≤ 0.05 into taxonomic units using the bClust function from the micropan R package (Snipen and Liland, 2015). We then measured the genetic distance between the representative genome of each species cluster (defined as the genome with the highest N50) and 79,226 non-contaminated complete and draft genomes downloaded from the NCBI FTP repository (ftp://ftp.ncbi.nlm.nih.gov/genomes/) on March 27th, 2017 (NCBI Resource Coordinators, 2016). Clusters with a Mash distance to NCBI genomes lower than 0.05 were assigned the taxonomy of the closest reference genome (we manually curated Mash results to assign a taxonomy to each cluster when NCBI taxonomies were incomplete or incorrect). All genome taxonomies are compiled in Table S2.

Comparison to the UHGG database

We compared the GMbC genome collection to the Unified Human Gastrointestinal Genome (UHGG) database, which comprises the largest set of human gut bacterial genomes, with the vast majority being metagenome-assembled genomes from uncultivated bacterial species (Almeida et al., 2021). We measured genomic distances between our representative genomes and all UHGG representative genomes with Mash, and counted the number of species that had not been previously sequenced or cultured, using a Mash threshold of 0.05.

Phylogenetic reconstructions

To reconstruct the phylogenomic tree of all 7,781 genomes, we first built a concatenated alignment of 47 nearly universal and single-copy ribosomal protein families. We used Diamond v0.8.22.84 (Buchfink et al., 2015) (with parameters blastx —more-sensitive -e 0.000001 —id 35 —query-cover 80) to BLAST all 7,781 proteomes against the RiboDB database (v1.4.1) of bacterial ribosomal protein genes (Jauffrit et al., 2016). We excluded proteins bL17, bS16, bS21, uL22, uS3 and uS4, as they were not sufficiently distributed across all genomes. In each RiboDB gene family, we excluded genomes that contained gene duplicates. Then, we aligned all protein families individually with Mafft v7.310 (Nakamura et al., 2018) (with parameter —auto). We filtered out misaligned sites using BMGE v1.12 (Criscuolo and Gribaldo, 2010) (with parameters -t AA -g 0.95 -m BLOSUM30) and concatenated all individual alignments using Seaview v4.7 (Gouy et al., 2010). We reconstructed the phylogenomic tree using FastTree v2.1.10 (with parameters -lg –gamma) (Price et al., 2010). To reconstruct phylogenetic trees of *B. vulgatus*, *B. ovatus*, *B. longum* and *A. muciniphila* (Figure 3 and Figure S3), we reconstructed the alignment of core protein-coding genes with Roary v3.11.2 (Page et al., 2015), removed recombining regions with Gubbins v2.2.0 (Croucher et al., 2015), extracted SNPs with SNP-sites v2.4.1 (Page et al., 2016) and inferred the tree with FastTree.

Detection and age of HGTs

In this study, we focus on transfers occurring between bacterial species, ignoring within-species gene recombination events. We looked for gene transfers that occurred between genomes of different bacterial species. We used Blast (blastn, v2.6.0) (Camacho et al., 2009) to systematically detect blocks of DNA that are shared by two genomes of different species. We retained blast hits with 100% similarity and that are larger than 500bp. To further increase the likelihood of looking at transfer events that occurred on timescales compatible with human lifetime, we focused many of our analyses on transferred blocks that are larger than 10kb. To remove putative contaminants from our set of blast hits when calculating HGT frequencies, we removed HGTs that involve contigs with both k-mer assembly coverage lower than 3 (as provided by SPAdes) and a relative read coverage lower than 0.2 compared to the average genome coverage in at least one of the two compared genomes.

Assuming a genome size in the order of 10^6 bp and molecular clock of 1 SNP/genome/year (Didelot et al., 2016; Drake, 1991; Duchêne et al., 2016; Zhao et al., 2019), HGTs larger than 500bp with > 99% similarity are consistent with transfer events that occurred between 0 and 10,000 years ago: this time interval corresponds to the time during which a 500bp sequence can accumulate a maximum of 1% sequence divergence, i.e., 5 SNPs. When considering 10kb+ HGTs with 100% similarity, it would take 1 year for a 10kb HGT to accumulate 10^{-2} SNPs, which corresponds to taking 100 years to experience 1 SNP and to be filtered out from our analysis. As such, our 10kb+ HGTs, which do not contain any mutations, correspond to events that occurred between 0 and ~100 years ago.

Calculating HGT counts and frequencies

To avoid inflating estimations of HGT counts and frequencies, we did not consider the absolute number of distinct blast hits between two genomes, as poor assembly or genomic processes, such as transposition, might result in splitting a single large HGT into many smaller apparent HGT events. Instead, we used a conservative approach to quantify HGTs that was previously published (Smillie et al., 2011), defining the HGT count as the number of between-species genome pairs that share at least one HGT (either one 500bp+ or 10kb+ HGT). To measure the frequency of HGT between two species, we then divided the HGT count by the total number of between-species genome pairs.

Simulation of HGT transmission across host generations

To simulate the fraction of 100% similar HGTs seen in the present generation 0 (HGT_0s) that would result from HGT events that occurred in past generation, we simulated a population of constant size with N species in each individual. As the median number of species in the microbiome of our sampled individuals is 187 based on Kraken2 metagenomic profiles, we fixed N = 200. At each generation, each pair of species had an H% probability to engage in HGT. In our dataset, the average proportion of species pairs engaging in HGT is 0.885. We then chose to fix H to 9%. In a previous report (Ferretti et al., 2018), the intergenerational mother-to-infant rate of strain transmission was found to be 16%. In our simulation, we compared a 16% rate of species transmission to the next host generation to a more extreme rate of 50%. So each species had a probability to transmit into the next generation drawn from one of two possible distributions:

- **B**(2,11), each species probability to transmit into offspring was chosen from a Beta distribution with parameters $\alpha = 2$ and $\beta = 11$
- **B**(2,2), each species probability to transmit into offspring was chosen from a Beta distribution with parameters $\alpha = 2$ and $\beta = 2$

We chose a Beta distribution to allow for some species to have an increased probability to transfer into later generations, even though the overall average was fixed at ∼16% for **B**(2,11) and 50% for **B**(2,2).

We then run the simulation across 5 generations, and recorded the generation of origin of each HGT. At the last generation (generation 0, corresponding to the generation at present time), we calculated the fraction of observed HGTs in the microbiome that occurred at each generation. We run 100 simulation replicates for each possible distribution of vertical transmission of strains into offspring. Simulations were run in Python.

Calculating gene gain and loss rates in the pangenome

We used Prokka gene annotations and Roary to reconstruct the core-genome alignment and the host individual-specific gene repertoires for *B. vulgatus*, *B. ovatus*, *B. longum* and *A. muciniphila* genomes that were longitudinally sampled in individual *am* (Poyet et al., 2019), and for *B. fragilis* genomes that were longitudinally sampled in individuals L01, L03, L04, L05, L06, L07 (Zhao et al., 2019). Note that individual *am* from (Poyet et al., 2019) and L01 from (Zhao et al., 2019) are the same individual. We used the following options with Roary: -e -n -z -i 90 -cd 95. We restricted our analysis to closely-related genomes that diversified within the host of origin upon colonization of the gut: genomes from individual am differed by 111, 42, 2,328 and 338 SNPs for *B. vulgatus*, *B. ovatus*, *B. longum* and *A. muciniphila*, respectively. When looking at genomes from all host individuals, isolate genomes differed by 68,746, 202,262, 51,064 and 33,793 SNPs, respectively. In addition, all *B. fragilis* genomes from the same individual differed by less than 100 SNPs, while those from different individuals differed by more than 10,000 SNPs (Zhao et al., 2019). This pattern suggests that we are only including closely-related genomes, limiting the potential impact of co-colonization of different major lineages or strain replacement on the analysis of the dynamics of gene gain and loss over time. We filtered genomes that had genome completeness as measured by CheckM below 99% out of the gene tables. For each species within each individual, we excluded genomes with low average coverage. With the final set of genomes, we checked whether the genome coverage was different across time points, as this could bias estimations of gene presence/absence profiles and gene gain/loss rates in pangenomes. We found that, for each species within each individual, genome coverage was homogeneous across time points (Kruskal-Wallis tests, see Figure S3J). Genome assemblies used to calculate gene gain and loss rates for each species within each individual is listed in Table S5.

Because of assembly errors, genes truly 'present' in a genome may not have been detected in the assembly by Prokka, and were later called 'absent' by Roary. We confirmed the presence and absence of genes in a given genome by mapping reads of each genome onto each gene sequence inferred by Prokka. For genes initially called 'absent' in a given genome but 'present' in other genomes, we used a representative sequence of this gene for mapping. To call for the presence of a gene in a genome, genes must be covered by a minimum of 20 reads over 90% of their length, and have a minimum relative coverage of 0.2 compared to the average genome coverage. To call 'present' a gene that was initially called 'absent', the gene was also required to have less than 30% ambiguous mappings to be called 'present', in addition to the criteria listed above.

To measure rates of gene gain and loss in the pangenome of each species between two time points, we identified the set of gene families that were absent in all genomes at initial sampling and present in at least 1 genome at the later time point. We repeated this procedure for all pairs of time points, and we normalized the rates of gene gain and loss to a number of events per year. We employed the same strategy for calculating rates of gene loss. When measuring differences in pangenome gene repertoires between two time points, we downsampled genomes at each time point to perform comparisons with the same number of genomes.

Analysis of metagenomic data

Metagenomic data were quality-filtered with Trim Galore v0.5.0 and Trimmomatic (same options as with isolate genomic sequencing data), dereplicated with FastUniq v1.1 (Xu et al., 2012) (default parameters) and mapped against the hg38 human reference genome with BWA v0.7.13 (Li and Durbin, 2009) (default options) to remove human reads. We used Kraken2 v2.0.8-beta (Wood et al., 2019) with default options and the Kraken2 database to call for taxonomies. We then used Bracken v2.5 (Lu et al., 2017) to refine Kraken2 taxonomic profiles at the species level, with the following options: -t 20 -k 35 -l 150. We rarefied the OTU (species) table, by down-sampling reads to the minimum number of reads among all samples. We measured beta-diversities with the Bray-Curtis dissimilarity metric using the 'vegdist' function from the 'vegan' R package (Oksanen et al., 2019). Metagenomic data were not used to reconstruct metagenome-assembled genomes, as only genome assemblies generated from isolate bacteria were analyzed in this study.

Measuring the abundance of isolate genomes

We measured average species abundances of isolates within each individual host. For species with more than five isolate genomes per individual, we randomly selected 5 genomes to compute the average abundance. For species with less than five isolate per individual, we used all isolates to calculate the average abundance. We mapped metagenomic data generated from the same individual host against each isolate genome, and used the per base coverage K, the average read length L, the size of each genome S and the total number of reads T in the shotgun data to calculate the relative abundance A of each genome in the metagenome with $A = (K*S/L) / T$. We used a threshold of 1% to define lowly and highly abundant bacteria. Results on the effect of abundance on HGT frequency (Figure 5A) hold true when using a 5% threshold to define high abundance (GLME, OR for lowly abundant species = 0.47; CI (95%) = 0.45 - 0.48; LRT, $\chi 2$ = 2668.1, p value = 1.5×10^{-71}).

Assigning Gram stain to bacterial species

We used Gram staining data from reference microbiology databases (ATCC, https://www.lgcstandards-atcc.org:443/en.aspx; DSMZ, https://www.dsmz.de/) & the Microbe Directory database (https://microbe.directory) and from publications characterizing the phenotype of bacterial isolates to assign a consensus Gram stain to each of our bacterial species. Species with contradictory Gram staining information or with unknown taxonomy were excluded from the analysis of the correlation between HGT frequency and cell wall architecture. Our data recapitulate what we know from the literature (Garrity, 2005; Krieg et al., 2011): Bacteroidetes are Gram-; Bifidobacterium are Gram+; Firmicutes are Gram+, to the exception of Negativicutes species, which are known diderm bacteria, and of a few other species; Fusobacterium are Gram-; Akkermansia are Gram-; Proteobacteria are Gram-.

Annotating transferred genes

Functional annotation followed the basic approach described previously (Brito et al., 2016). Briefly, CDS were assigned to all 500bp+ HGTs using Prodigal v2.6.3 (Brito et al., 2016; Hyatt et al., 2010) in metagenome mode to capture gene fragments. The resultant CDS were dereplicated and clustered at 90% nucleotide identity using vsearch v2.3.4 (Rognes et al., 2016). These gene centroids were used for subsequent functional annotation steps. Both eggNOG-mapper (Huerta-Cepas et al., 2017) and InterProScan v5.36-75.0 (Jones et al., 2014) were used to assign putative function predictions to gene centroids. For additional classification of antibiotic resistance genes and carbohydrate active enzymes, hmmer3 v3.1b2 (Mistry et al., 2013) was used with the Resfam (Gibson et al., 2015) and dbCAN (Yin et al., 2012) hmm databases with a cutoff e-value of $1e^{-5}$ and score of 22. Text mining with a set of regular functional annotations that we previously used (Brito et al., 2016) was employed to determine the assignment of genes into the following categories: phage, plasmid, transposons, and antibiotic resistance.

To investigate whether, within people, bacterial species engage in the transfer of gene functions that may impact bacterial metabolism or host physiology, we looked at within-person transferred genes involved in antibiotic resistance (ARG), carbohydrate degradation (CAZyme) and virulence. We chose these functions in part because they seemed likely to reflect relevant selective pressures in the human host, and also because there exist well curated databases of annotated genes. In Figure 3D ('Upset' plot), each row corresponds to a function set, and each column corresponds to an interaction configuration. Empty cells (light-gray) indicate that the set is not part of the intersection, and filled (black) cells show sets that participate in the intersection. Barplots on the top and right of the matrix layout show absolute counts of species pairs for each intersection and each set, respectively.

QUANTIFICATION AND STATISTICAL ANALYSES

When the R output of a *p value* calculation equalled to 0, we used the smallest double-precision machine number, which is $2.2*10^{-308}$. Such p values are shown with an asterisk in figures.

Comparing HGT frequencies and counts

Statistical analyses were performed in R. When comparing HGTs between two categories, e.g., within-person versus between-people or Urban industrialized versus Rural non-industrialized, the numbers of genome and individual pairs for any pair of bacterial species that were sampled are different between the two categories. This difference in sampling could interfere with comparisons of HGT frequencies. To correct for differences in sampling, we employed the following approach. Consider the comparison of within-person to between-people HGTs: we calculated, for each species pair, the observed within-person HGT count (corresponding to the number

of within-person genome comparisons with at least 1 HGT) and the expected within-person HGT count based on the between-people HGT frequency of the same species pair. We then summed observed and expected HGT counts across all species pairs and compared the observed total HGT count within individual people to its expected value based on the amount of transfer seen between individuals, and calculated a p value using the Poisson distribution (ppois R function). The same approach was used to compare HGT counts of the same species pairs found in different cohorts that have different lifestyles (Figure 4), for instance to compare counts of HGT in the Urban & Industrialized cohort to the Rural & Non-industrialized cohort. This approach allows us to control for differences in the number of genome, species and individual pairs sampled between two compared cohorts (within-person versus between-people or Urban & Industrialized versus Rural & Non-industrialized). Note that when measuring the effect of lifestyle on HGT, observed HGTs, expected HGTs and p values were calculated for each pair of cohorts (4 lifestyle categories, 6 cohort pairs in total). Also, as this analysis is a-symmetrical, we also performed all our tests in the other direction, i.e., testing whether the observed between-people HGT count is *lower* than the expected between-people HGT count based on within-person HGT frequencies (118,210 versus 671,160, *p value* $< 2.2*10^{-308}$); and whether the observed Rural & Industrialized HGT count is *lower* than the expected count based on Urban & Industrialized HGT frequencies (42,254 versus 66,276, *p value* $< 2.2*10^{-308}$).

We also controlled for the effect of including multiple genome pairs of the same species pairs sampled in individuals when comparing total observed and expected HGT counts. We downsampled our dataset by randomly drawing a single genome pair per species pair and per individual pair. We run this control for the comparison of within-person to between-people HGTs, and for the comparison of Urban & Industrialized (UI) to Rural & Non-industrialized (RN) HGTs. For each comparison, we run 100 random replicates. For each replicate, we calculated the total observed and expected HGT counts for the within-person category or the UI group, as described above. We then compared the distributions of observed and expected HGTs with a Welsh t test. Results are shown in Table S4.

Calculating the frequency of transferred genes within bacterial populations
The population frequency of a given mobile gene carried by a 10kb+ HGT detected in a given species and in a given individual was calculated by counting the number of genomes carrying this mobile gene, divided by the total number of genomes of this species in this individual. Only species with a minimum of 10 genomes in each individual were included.

Controlling for the effect of phylogeny on within-person versus between-people HGT
To measure the difference between within-person and between-people HGT across phylogenetic distance bins (Figure 3B), we compared for each separate bin the total observed within-person HGT count across all species pairs to its expected count value based on the between-people HGT frequencies of the same species pairs in that bin, with a Poisson distribution. P values were then combined into a single p value with Fisher's method ('sumlog' function from the 'metap' R package).

Controlling for the effect of *in vitro* culturing
To control for the effect of *in vitro* culturing on the estimation of within-person HGTs and its comparison with between-people HGTs, we used our set of 10kb+ HGTs to test (i) whether within-person HGTs are more frequent when genome pairs are sampled from the same versus different culturing plates and (ii) for genome pairs isolated from the same plate, whether HGTs are more frequent when genome pairs are sampled from a media containing antibiotics. These tests control for (i) HGTs that may occur during the culturing on the plate and (ii) HGTs that may be triggered by antibiotics present in the media. We compared HGTs for all bacterial species pairs from each individual host that were sampled in both categories of each of the aforementioned variables being tested. As we are comparing HGTs for genome pairs from the same species pairs sampled from the same individual, we do not need to control for differences in bacterial phylogenetic distances or abundances. We compared the total observed HGT counts for genome pairs cultured within the same plate to its total expected value based on the HGT frequency of genome pairs of the same species being cultured from different plates, using a Poisson distribution. We used the same approach for genome pairs being grown on antibiotic-containing media versus without antibiotics. We also correlated observed to expected HGT counts for each species pair using a Pearson correlation. Finally, we also compared within-plate to between-plate HGT frequencies and with-antibiotics versus without-antibiotics HGT frequencies using paired Wilcoxon tests. All results are shown in Table S4.

Permutation test to compare HGTs from populations with different lifestyles
We also used a permutation test to compare HGTs in two cohorts of different lifestyles. We defined the statistic S = (HGTcounts_observed - HGTcounts_expected) / HGTcounts_expected. For the more industrialized and urban cohort, HGTcounts_observed > HGTcounts_expected. We tested if the difference between observed and expected counts is higher with real data than under a null hypothesis. We computed the null distribution of S by rearranging the lifestyle labels of either each individual participant, or each pair of participant before calculating average HGT frequencies. The value of S obtained with real data was then compared to the null distribution to calculate the p value. Null distributions of S for these tests are shown in Figure S4.

Measuring the effect of bacterial phylogeny, abundance and cell-wall architecture on HGT
The effect of phylogeny on HGT frequency was measured using Generalized Linear Mixed Effects (GLME) models, assuming an intercept that is different for each pair of species. We also accounted for the effects of bacterial abundance and cell-wall architecture

(Gram-negative versus Gram-positive) in the models. We used the lme4 R package (Bates et al., 2015) (glmer function) to fit the GLME models, and used Likelihood Ratio Tests (with the lmtest package and the lrtest function; Zeileis and Hothorn, 2002) to calculate the *p value* for phylogeny. Confident intervals for odds ratios were calculated with the Wald method.

We defined the following variables:

- phylogeny: Continuous variable. Phylogenetic distance between two species derived from the phylogenomic tree shown in Figure 2A.
- abundance: Discrete variable. Abundance category for each pair of species in each sampled host individual, derived from the abundance category of each individual species. We used a threshold of 1% relative abundance to classify species as highly or lowly abundant in each individual.
- gram_staining: Discrete variable. Gram staining category for each pair of species derived from the individual Gram staining of each individual species.
- hgt_freqs: Continuous variable. Average within-person HGT frequency for each individual species pair. Average within-person HGT frequencies were calculated for each population separately, to account for population-level differences.
- species_pairs: Discrete variable. Names of species pairs. Because we calculated within-person HGT frequencies on a per-population basis, a given species pair can be represented multiple times in the model. We accounted for this by considering the variable species_pairs as a random effect term in the GLME models.

We fitted the following models, with HGT frequencies either derived from the dataset of 10kb+ HGTs or from the dataset of 500bp+ HGTs:

model1 = glmer(hgt_freqs ~phylogeny + abundance + gram_staining + (1|species_pairs), family = "binomial")
model2 = glmer(hgt_freqs ~abundance * gram_staining + (1|species_pairs), family = "binomial")

To assess whether phylogeny is significantly contributing to HGTs, we performed the following LRT:

Phylogeny: LRT_phylogeny = lrtest(model1, model2)

To measure the effect of lifestyle on HGT with the dataset of 500bp+ HGTs, while controlling for the effects of phylogeny, abundance and cell-wall architecture, we defined the discrete variable 'lifestyle' as the level of host industrialization associated with the sampled species pair (i.e., 'industrialized' or 'non-industrialized'), and run the following GLME models:

model3 = glmer(hgt_freqs ~phylogeny + abundance + gram_staining + lifestyle + (1|species_pairs), family = "binomial")
model4 = glmer(hgt_freqs ~abundance + gram_staining + lifestyle + (1|species_pairs), family = "binomial")
model5 = glmer(hgt_freqs ~phylogeny + gram_staining + lifestyle + (1|species_pairs), family = "binomial")
model6 = glmer(hgt_freqs ~phylogeny + abundance + lifestyle + (1|species_pairs), family = "binomial")
model7 = glmer(hgt_freqs ~phylogeny + abundance + gram_staining + (1|species_pairs), family = "binomial")

We run the following LRTs to evaluate the contribution of each factor to HGT:

Phylogeny: LRT_phylogeny = lrtest(model3, model4)
Abundance: LRT_abundance = lrtest(model3, model5)
Cell-wall architecture: LRT_cell-wall = lrtest(model3, model6)
Lifestyle: LRT_lifestyle = lrtest(model3, model7)

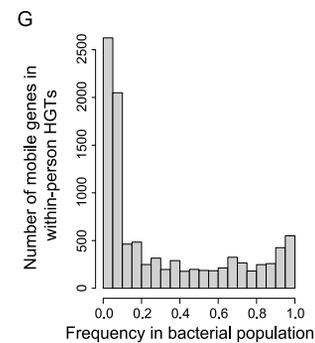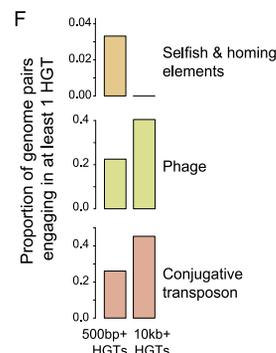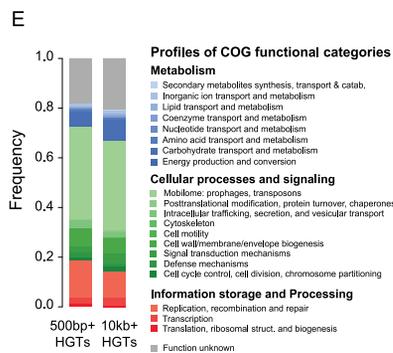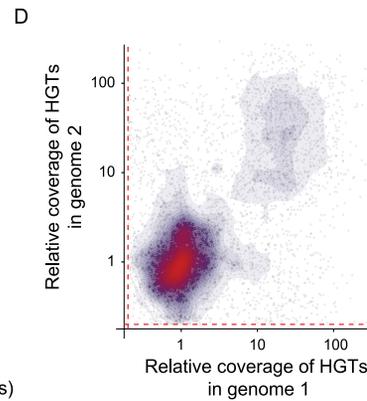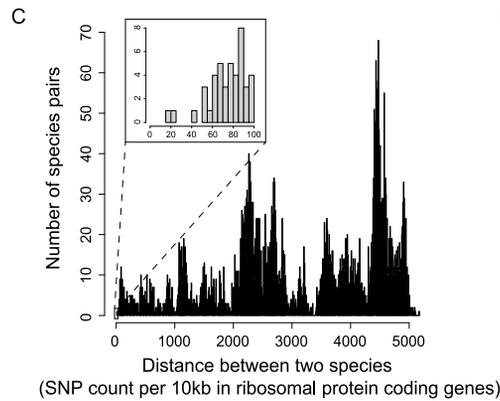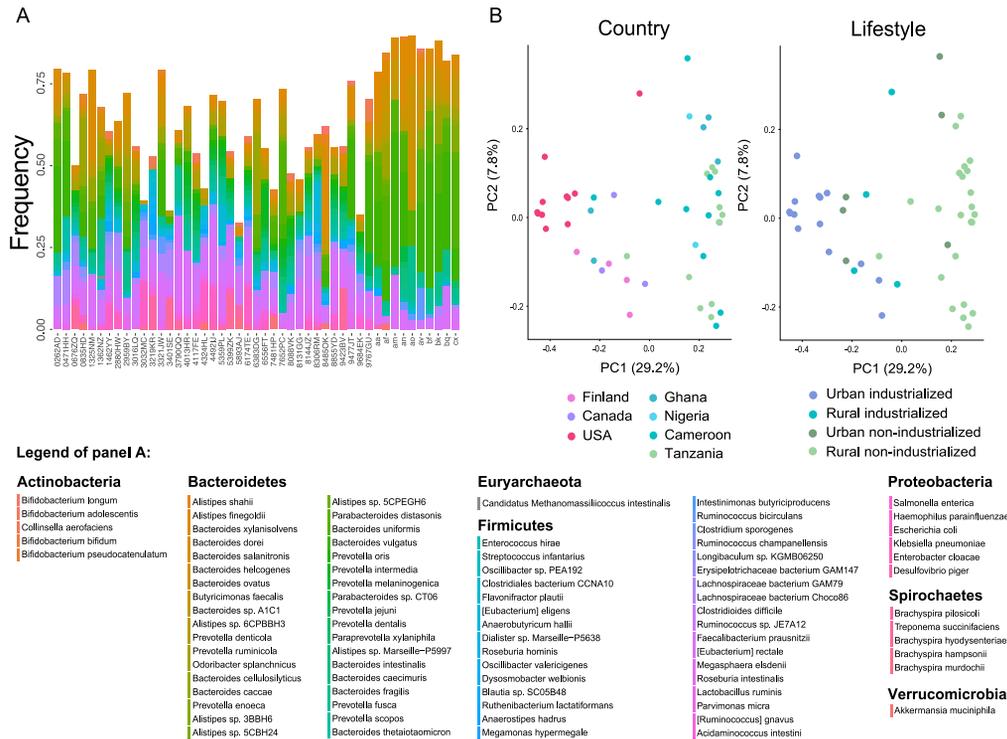### Comparing functional profiles of HGTs

Profiles of COG functional categories were compared using a chi-square Goodness-of-fit test (chisq.test function). HGT frequencies of phage, plasmid, transposon, ARG, CAZyme and Virulence genes were compared between host populations of different lifestyles (Figure 6) using two-proportions Z-tests (prop.test function), and a Bonferroni correction for multiple tests (p.adjust function).

LOESS regressions

LOESS regressions were calculated with the ggplot2 package (Figures 3 and 5). HGT frequencies at phylogenetic distances lower than the smallest between-species distances (left part of the curves) are extrapolated. Bands represent confidence intervals calculated from the standard errors.

Supplemental figures

Legend of panel A:

Actinobacteria

Bifidobacterium longum
Bifidobacterium adolescentis
Collinsella aerofaciens
Bifidobacterium bifidum
Bifidobacterium pseudocatenulatum

Bacteroidetes

Alistipes shahii
Alistipes finegoldii
Bacteroides xylanisolvens
Bacteroides dorei
Bacteroides salanitronis
Bacteroides helcogenes
Bacteroides ovatus
Butyricimonas faecalis
Bacteroides sp. A1C1
Alistipes sp. 6CPBBH3
Prevotella denticola
Prevotella ruminicola
Odoribacter splanchnicus
Bacteroides cellulosilyticus
Bacteroides caccae
Prevotella enoeca
Alistipes sp. 3BBH6
Alistipes sp. 5CBH24

Alistipes sp. 5CPEGH6
Parabacteroides distasonis
Bacteroides uniformis
Bacteroides vulgatus
Prevotella oris
Prevotella intermedia
Prevotella melaninogenica
Parabacteroides sp. CT06
Prevotella jejuni
Prevotella dentalis
Paraprevotella xylaniphila
Alistipes sp. Marseille−P5997
Bacteroides intestinalis
Bacteroides caecimuris
Bacteroides fragilis
Prevotella fusca
Prevotella scopos
Bacteroides thetaiotaomicron

Euryarchaeota

Candidatus Methanomassiliicoccus intestinalis

Firmicutes

Enterococcus hirae
Streptococcus infantarius
Oscillibacter sp. PEA192
Clostridiales bacterium CCNA10
Flavonifractor plautii
[Eubacterium] eligens
Anaerobutyricum hallii
Dialister sp. Marseille−P5638
Roseburia hominis
Oscillibacter valericigenes
Blautia sp. SC05B48
Dysosmobacter welbionis
Ruthenibacterium lactatiformans
Anaerostipes hadrus
Megamonas hypermegale

Intestinimonas butyriciproducens
Ruminococcus bicirculans
Clostridium sporogenes
Ruminococcus champanellensis
Longibaculum sp. KGMB06250
Erysipelotrichaceae bacterium GAM147
Lachnospiraceae bacterium GAM79
Lachnospiraceae bacterium Choco86
Clostridioides difficile
Ruminococcus sp. JE7A12
Faecalibacterium prausnitzii
[Eubacterium] rectale
Megasphaera elsdenii
Roseburia intestinalis
Lactobacillus ruminis
Parvimonas micra
[Ruminococcus] gnavus
Acidaminococcus intestini

Proteobacteria

Salmonella enterica
Haemophilus parainfluenzae
Escherichia coli
Klebsiella pneumoniae
Enterobacter cloacae
Desulfovibrio piger

Spirochaetes

Brachyspira pilosicoli
Treponema succinifaciens
Brachyspira hyodysenteriae
Brachyspira hampsonii
Brachyspira murdochii

Verrucomicrobia

Akkermansia muciniphila

(legend on next page)

Figure S1. Sampled microbiomes and horizontal gene transfers, related to Figures 1 and 2
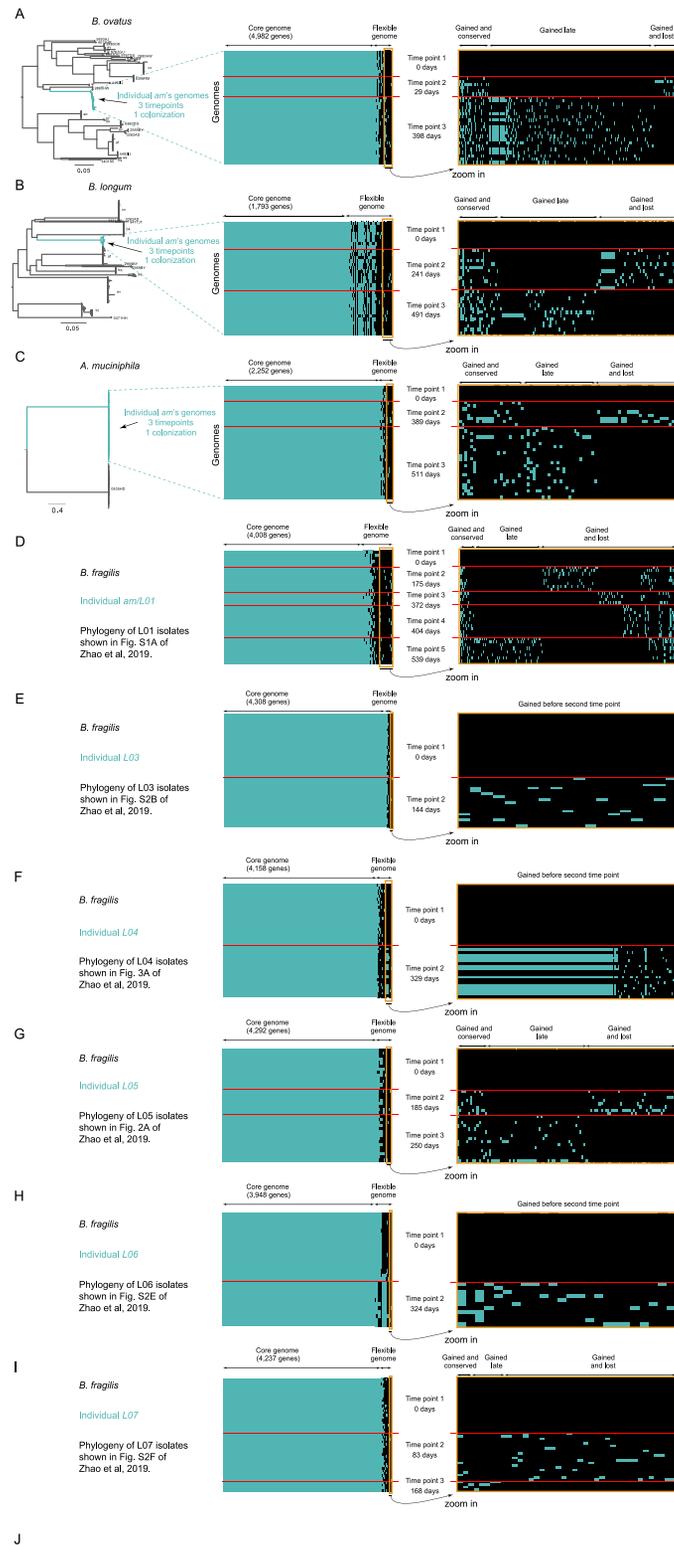
(A) Microbiome profiles of the 48 individuals, derived from metagenomic sequencing data and Kraken2 abundances. Only species with abundances higher than 1% are shown. (B) Microbiome compositions of the 48 individuals in our cohort cluster by geography (left) and lifestyle (right) (Adonis test, *p value* = 0.001). Bacterial species compositions were derived from metagenomic data, using Kraken2. (C) Distribution of SNP counts across vertically-transmitted ribosomal protein coding genes. HGTs were called by detecting 100% similar blocks of DNA larger than 500bp or 10kb occurring in genomes of different bacterial species. To confirm that this workflow detects true HGTs and not scenarios of vertical inheritance along bacterial lineages, we determined the distribution of SNPs in vertically-transmitted and slowly-evolving genes. For each species pair in which we found HGT candidates, we calculated the number of SNPs between shared ribosomal genes, and normalized this count to a number of SNPs per 10kb. On average, 3,146 SNPs per 10kb exist in ribosomal genes of two different species, far more than the threshold that we used to conserve blast hits in our dataset (0 SNPs). To obtain the number of SNPs per 500 bp that is relevant to our second length criteria to filter blast hits (500bp), simply divide numbers by a factor of 20. Only 1 species pair out of 5,304 has a number of SNPs per 500bp below 1 (n = 0.94). (D) Relative coverages of each HGT. Our pipeline detected a total of 5,267,297 500bp+ HGTs. The coverage of each HGT in all isolate genome pairs in which they were detected was calculated using Bowtie2 and was compared to the average coverage of each genome. In this density plot, each dot is an HGT, and relative coverages are shown on a log scale. Density of points is represented along a gradient color from blue (low density) to red (high density). The median relative coverage across all 5,267,297 500bp+ HGTs is 1.13. Dashed lines show the threshold (0.2) used to exclude HGTs from the dataset. The vast majority of HGTs have a relative coverage compared to the rest of the genome around 1. (E) CDSs were called using Prodigal on the set of 5,267,297 500bp+ HGTs, and on the set of 200,458 10kb+ HGTs. CDSs were annotated with eggNOG and Interproscan. In this figure, COG functional categories are represented. (F) Proportion of genome pairs engaging in HGTs that include genes annotated with selfish element, phage and conjugative transposon functions in the set of 500bp+ and 10kb+ HGTs. HGT counts for each function category represents the number of genome pairs involved in at least 1 HGT containing at least 1 gene annotated with one of the three functions. We calculated the proportion by dividing these HGT counts by the total number of genome pairs. The category of Selfish and homing elements include HGTs with genes annotated with intein or intron (e.g., Group II introns) functions. (G) The population frequency of a given mobile gene detected in a given species in a given individual was calculated by counting the number of genomes carrying this mobile gene, divided by the total number of genomes of this species in this individual. Only species with a minimum of 10 genomes were considered. We found that the vast majority of these (very recently) transferred genes segregate at low frequency and are not fixed in bacterial populations.
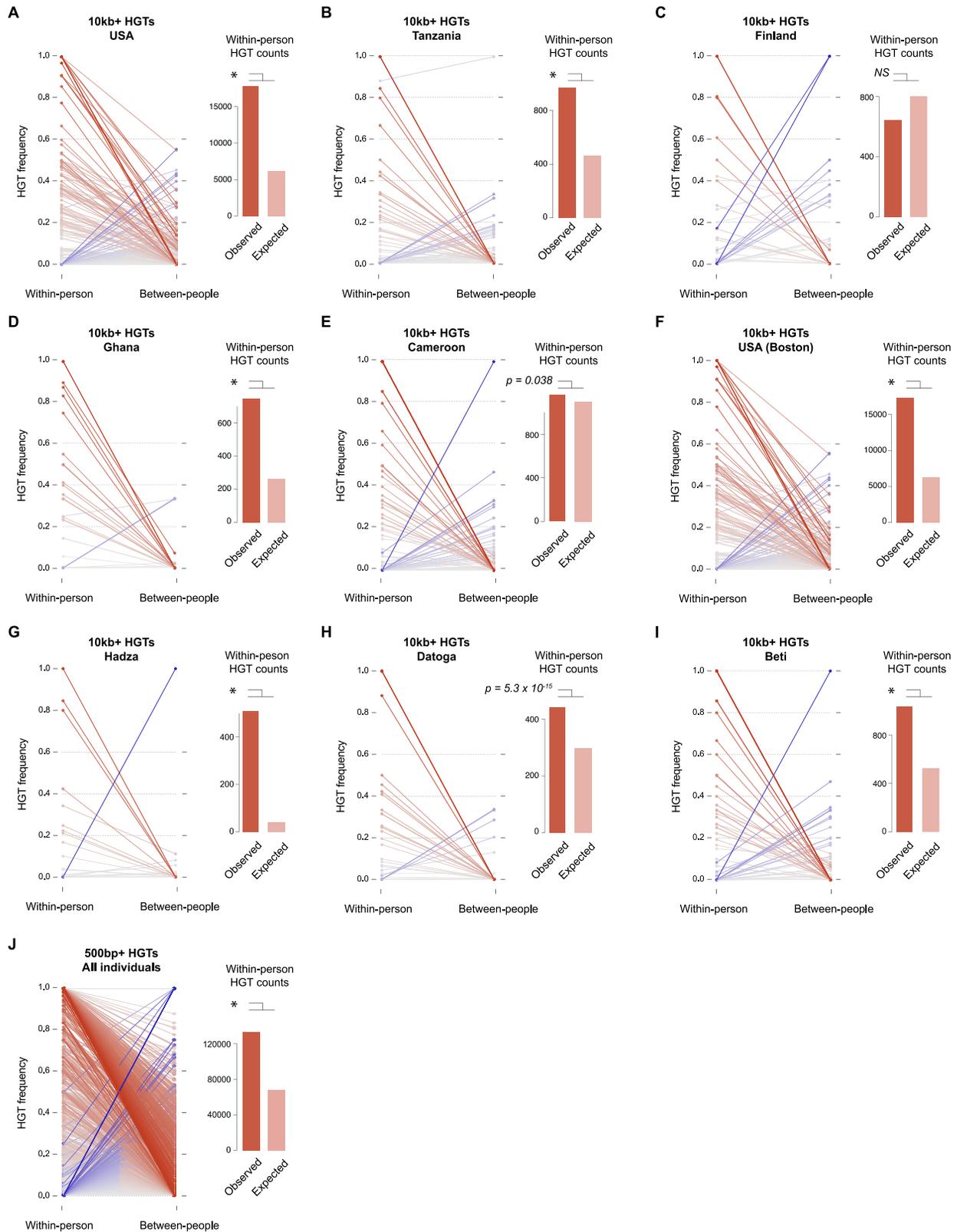
(legend on next page)

Figure S2. Extensive within-person gene transfers in the gut microbiome is found when looking at different resolutions of geography, human population and size of HGTs, related to Figure 3A

(A–E) HGT frequencies calculated within and between people are shown for each country with at least 4 sampled individuals (USA (A), Finland (B), Tanzania (C), Ghana (D) and Cameroon (E)). Canada and Ghana are excluded (N individuals < 4). HGT frequencies were calculated with the set of 10kb+ HGTs. Each solid line represents a bacterial species pair sampled in both within and between individuals. Differences in HGT frequency are colored along a gradient from gray (no difference) to red (within-people HGT frequency is higher than between-people) or from gray to blue (between-people HGT frequency is higher than within-people), darker colors representing higher differences. The barplot shows the observed total HGT in bacterial species pairs found within individual people (left bar), compared to its expected value (right bar) based on HGT frequencies of the same species pairs found between people. Observed and expected HGTs were compared with a Poisson distribution to calculate the p value of a one-sided test (*: $p\ value < 2.2x10^{-308}$). (F–I) HGT frequencies calculated within-person and between-people are shown for each ethnic group with at least 4 sampled individuals (Multi-ethnic cohort in the Boston area (F), Hadza hunter-gatherers in Tanzania (G), Datoga pastoralists in Tanzania, (H) and Beti farmers in Cameroon (I)). Ashanti, Fante, Yoruba, Ahafo, Ga, Northern Cheyenne, Sami and Inuit people are excluded (N individuals < 4). As in panels A–E, line plots show HGT frequencies for each species pairs sampled both within-person and between-people, and barplots show observed and expected numbers of within-person HGTs (*: $p\ value < 2.2x10^{-308}$). (J) Comparison of within-person and between-people HGT frequencies calculated from the whole set of 5,267,297 500bp+ HGTs.

Figure S3. Within-person gene gains in bacterial pangenomes, related to Figure 3E

Isolates of *Bacteroides ovatus* (A), *Bifidobacterium longum* (B) and *Akkermansia muciniphila* (C) were longitudinally sampled in individual *am* (USA) (Poyet et al., 2019). Isolates of *Bacteroides fragilis* (D–I) were longitudinally sampled in individuals L01, L03, L04, L05, L06 and L07 in another previous study (Zhao et al., 2019). Note that individuals *am* from Poyet et al. (2019) and L01 from Zhao et al. (2019) are the same individual. For each species, a core-SNP phylogenetic tree was reconstructed to depict the relationship between all isolates of this species that we have in our genome collection. In A), B) and C), blue clades show the isolates that were sampled from individual *am*. The IDs of the other individual hosts are shown next to each corresponding clade of isolates. Trees for *B. fragilis* isolates in individuals *L01*, *L03*, *L04*, *L05*, *L06* and *L07* are shown in Zhao et al. (2019) - corresponding figures are indicated on the left of panels D) to I). All trees strongly suggest that isolates originate from a single colonization event and diversified within each sampled individual. In all panels, middle and right heatmaps show gene presence/absence in all isolate genomes (rows), sorted by sampling times. The number of days elapsed since original sampling are shown for each time point. In each panel, the heatmap on the right is a zoom-in on the set of gene families (orange box in the middle panel) that were absent in the pangenome of the first time point, and gained in the pangenome later in time within each individual. Table in panel J) shows the comparison of the genome coverage across time points for each species in each individual (Kruskal-Wallis test). In all cases, the genome coverage is not statistically different across time points.

Null distributions of S

Shuffling lifestyle of pairs of individuals   Shuffling lifestyle of individuals

$$\text{Statistic S} = \frac{(HGT_{obs} - HGT_{exp})}{HGT_{exp}}$$
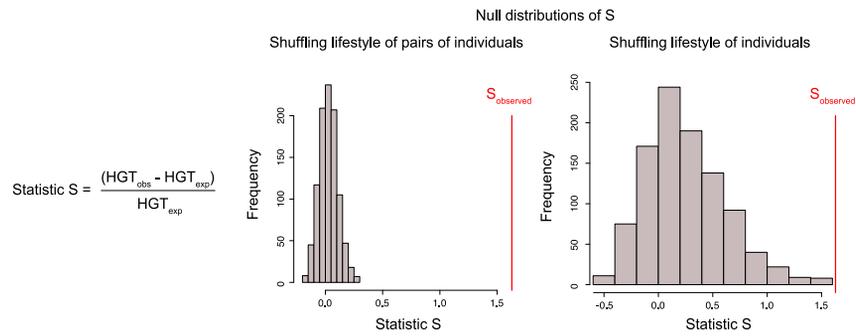

Figure S4. The signal for elevated HGT in urban industrialized populations is robust to heterogeneities in HGT across individuals, related to Figure 4B

Permutation tests to compare HGT amounts in the urban industrialized (UI) cohort to HGTs in the rural non-industrialized (RN) cohort. Expected HGTs for the urban industrialized cohort are based on the HGT frequencies of the same species pairs found in the RN cohort. HGT frequencies were calculated by averaging HGT frequencies across all pairs of individuals within each cohort (both within and between-people pairs). We defined the statistic S as in the figure, and we calculated S_{obs} from real data (red vertical lines). We compared this statistic to a null distribution obtained by shuffling either the lifestyle of pairs of individuals (left histogram) or the lifestyle of individuals (right histogram) before calculating averages of HGT frequencies. For each permutation, cohort sizes (number of people pairs) were fixed to observed sizes. 1,000 permutations were performed in each case. Both p values are < 0.001.
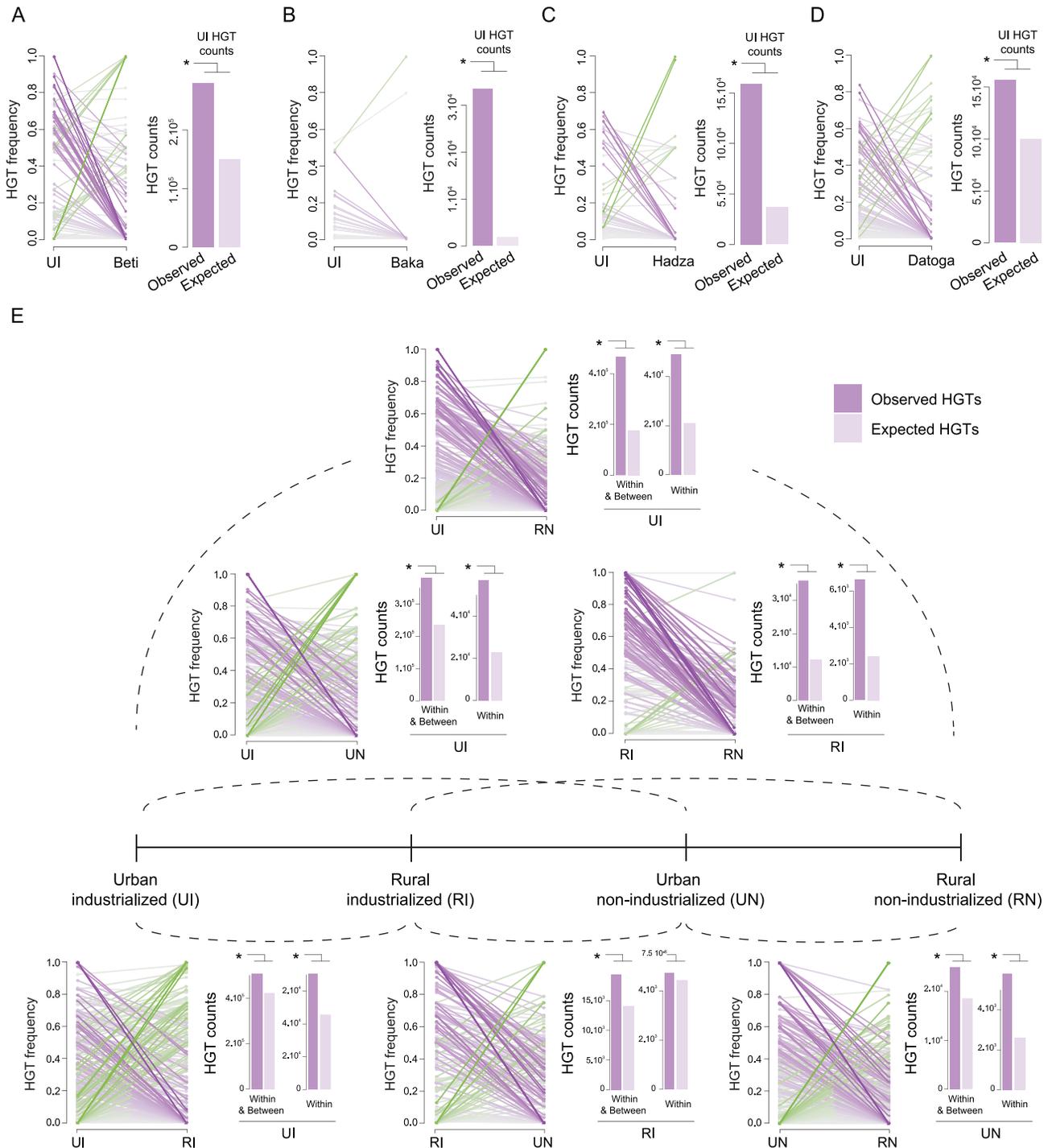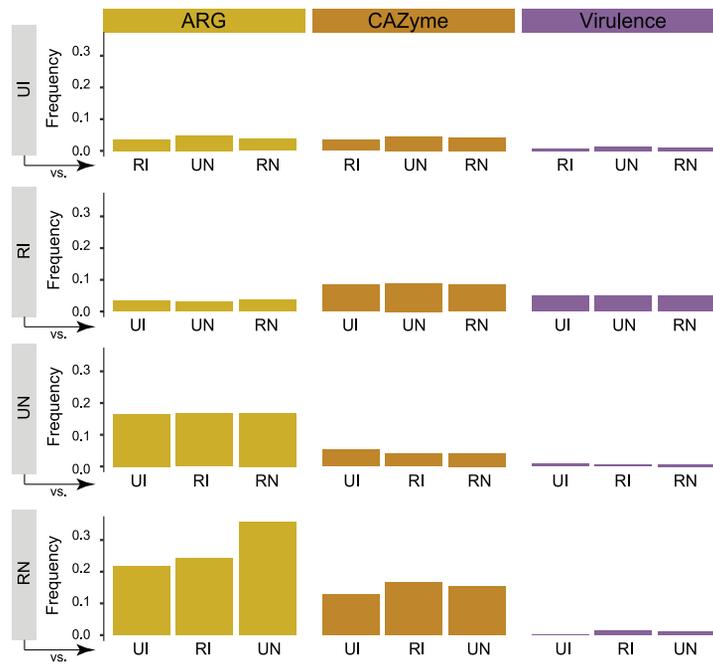
Figure S5. Elevated HGT frequency in the gut microbiome of individuals living in industrialized and urban populations, related to Figures 4B and 4C
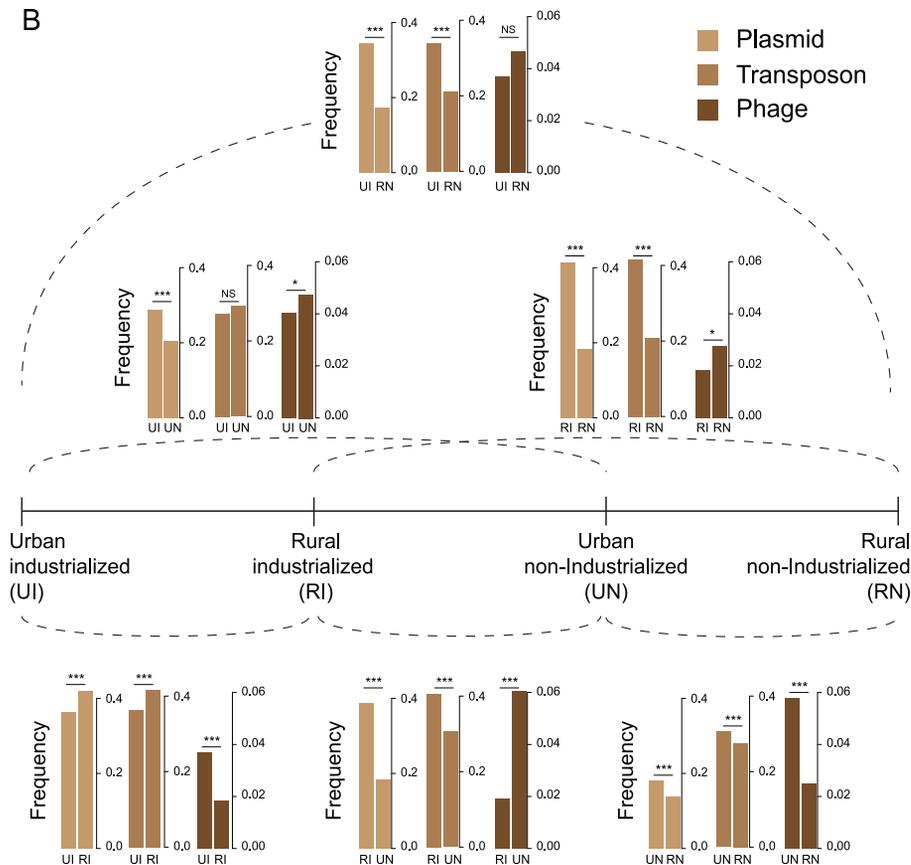
Gut bacterial species in urban industrialized (UI) individuals exchange genes at higher frequency than in rural non-industrialized (RN) communities (Figure 4B). This effect holds true when comparing the UI cohort to every individual rural non-industrialized ethnic group that have specific lifestyles (Beti, farmers (A); Baka, hunter-gatherers & farmers (B); Hadza, hunter-gatherers (C); Datoga, pastoralists (D). See legend of Figure 4B for legends of line and bar plots (panels A to D). (E) This panel presents raw results complementing Figure 4C in the main text, which shows the comparison of HGT frequencies of all species pairs shared between pairs of cohorts having different lifestyles, along a gradient of industrialization and urbanization. See legend of Figure 4B for legends of line and bar plots. For each lifestyle comparison, the left barplot shows HGT counts when considering both within and between-people HGTs, and the one on the right is for within-people HGTs only (*: *p value < 2.2x10^{-308}*). Ratios of observed versus expected HGT counts were computed for each cohort pair, and these ratios were compared to the Industrialized & Urban cohort to produce the barplot shown in Figure 4C.
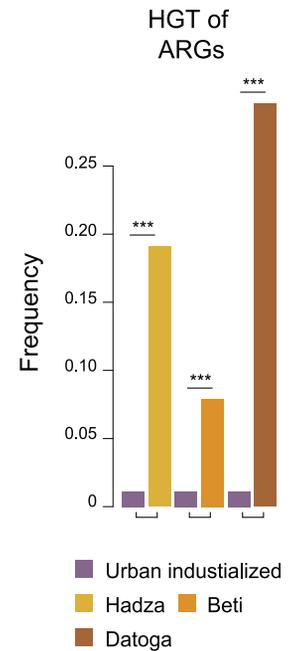
(legend on next page)

Figure S6. Transferred functions across host lifestyles, related to Figure 6

(A) Homogeneity of frequencies for HGT functions across pairs of bacterial species in the gut microbiome. When comparing functions of transferred coding sequences between two cohorts (e.g., Urban & Industrialized versus Rural & Non-industrialized), we looked at functions exchanged across pairs of species of our isolate collection that are shared by the two cohorts. Consequently, pairs of species being compared are different across pairs of cohorts. We used the Levene's test for Homogeneity of Variance to assess whether, for any given cohort, the different sampling of species pairs across pairwise cohort comparisons resulted in differences in frequencies of transferred ARG, CAZyme and virulence genes. Overall, we found that the frequency of each these three functions is homogeneous across cohort comparisons (e.g., UI versus RI, UI versus UM and UI versus RN) (df = 11, F value = 1.5643, p value = 0.17). In this figure, the three functions are represented in columns. Each row represents the frequency of transferred genes for a given cohort (e.g., UI - Urban & Industrialized cohort) when it is compared to the three other cohorts (e.g., IR, NU and NR). (B) Profiles of frequencies for plasmid, transposon and phage genes were compared for all lifestyle pairs using two-proportions Z-tests followed by a Bonferroni correction for multiple tests (*p values < 0.05; **p values < 0.01; ***p values < 0.001. For a given lifestyle pair, frequencies were averaged across all pairs of individuals in each lifestyle category. In addition, for any given cohort comparison, frequencies of HGT functions were calculated using only species pairs that were sampled in both cohorts. Genes involved in plasmid and transposon functions are frequently transferred across all cohorts, suggesting that the majority of recent HGTs occur through the exchange of these genetic systems. Overall, we observe a trend for an increased frequency of transferred plasmids and transposons in industrialized and/or urban cohorts as compared to non-industrialized and/or rural cohorts. (C) We compared the frequency of transferred antibiotic resistance genes in the Urban & Industrialized cohort to three other rural and non-industrialized cohorts having different lifestyles: the Hadza, who are Hunter-gatherers, the Beti, who are farmers, and the Datoga, who are pastoralists, and who frequently use antibiotics for their livestocks. We observe that all rural and non-industrialized cohorts consistently exchange ARG more frequently than in the urban and industrialized cohort (see Figure 6), and that the Datoga is the population that recently experienced the highest frequency of ARG transfers.